Journal Pre-proof

Advanced qEEG analyses discriminate between dementia subtypes

Masha Burelo, Jack Bray, Olga Gulka, Michael Firbank, John-Paul Taylor, Bettina Platt

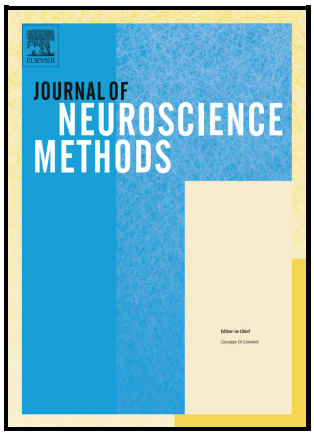

PII: S0165-0270(24)00140-7

DOI: https://doi.org/10.1016/j.jneumeth.2024.110195

Reference: NSM110195

To appear in: *Journal of Neuroscience Methods*

Received date: 9 November 2023
Revised date: 3 June 2024
Accepted date: 10 June 2024

Please cite this article as: Masha Burelo, Jack Bray, Olga Gulka, Michael Firbank, John-Paul Taylor and Bettina Platt, Advanced qEEG analyses discriminate between dementia subtypes, *Journal of Neuroscience Methods,* (2024) doi:https://doi.org/10.1016/j.jneumeth.2024.110195

This is a PDF file of an article that has undergone enhancements after acceptance, such as the addition of a cover page and metadata, and formatting for readability, but it is not yet the definitive version of record. This version will undergo additional copyediting, typesetting and review before it is published in its final form, but we are providing this version to give early visibility of the article. Please note that, during the production process, errors may be discovered which could affect the content, and all legal disclaimers that apply to the journal pertain.

© 2024 Published by Elsevier B.V.

Journal Pre-proof

Advanced qEEG analyses discriminate between dementia subtypes

Masha Burelo[1], Jack Bray[1], Olga Gulka[1], Michael Firbank[2], John-Paul Taylor[2], Bettina Platt[1]*

[1] School of Medical Sciences, Institute of Medical Sciences, University of Aberdeen, Foresterhill, Aberdeen, AB25 2ZD Scotland, United Kingdom.

[2] Translational and Clinical Research Institute, Newcastle University, NE1 7RU Newcastle upon Tyne, United Kingdom.

*Corresponding author: Bettina Platt, Institute of Medical Sciences, University of Aberdeen, Foresterhill, Aberdeen, AB25 2ZD Scotland, United Kingdom, Tel.: +44 1224 437402, E-mail: b.platt@abdn.ac.uk

Highlights:

- Standard FFT spectra discriminated between synucleinopathies and controls during eyes open conditions.
- Autoregressive (AR) modelling identified fewer spectral differences between cohorts but delivered enhanced spectral smoothing.
- Slowing of the dominant frequency (4-15 Hz range) differentiated between synucleinopathies vs controls during eyes closed only.
- Combining AR spectra with FOOOF yielded robust differences of periodic parameter between all conditions vs controls in eyes open and closed.
- Aperiodic EEG parameters (1-45 Hz) achieved the most superior discrimination for all channels and conditions.

Journal Pre-proof

Abstract

Background: Dementia is caused by neurodegenerative conditions and characterized by cognitive decline. Diagnostic accuracy for dementia subtypes, such as Alzheimer's Disease (AD), Dementia with Lewy Bodies (DLB) and Parkinson's Disease with dementia (PDD), remains challenging.

Methods: Here, different methods of quantitative electroencephalography (qEEG) analyses were employed to assess their effectiveness in distinguishing dementia subtypes from healthy controls under eyes closed (EC) and eyes open (EO) conditions.

Results: Classic Fast-Fourier Transform (FFT) and autoregressive (AR) power analyses differentiated between all conditions for the 4-8 Hz theta range. Only individuals with dementia with Lewy Bodies (DLB) differed from healthy subjects for the wider 4-15 Hz frequency range, encompassing the actual dominant frequency of all individuals. FFT results for this range yielded wider significant discriminators vs AR, also detecting differences between AD and DLB. Analyses of the inclusive dominant / peak frequency range (4-15 Hz) indicated slowing and reduced variability, also discriminating between synucleinopathies vs controls and AD. Dissociation of periodic oscillations and aperiodic components of AR spectra using Fitting-Oscillations-&-One-Over-F (FOOOF) modelling delivered a reliable and subtype-specific slowing of brain oscillatory peaks during EC and EO for all groups. Distinct and robust differences were particularly strong for aperiodic parameters, suggesting their potential diagnostic power in detecting specific changes resulting from age and cognitive status.

Conclusion: Our findings indicate that qEEG methods can reliably detect dementia subtypes. Spectral analyses comprising an integrated, multi-parameter EEG approach discriminating between periodic and aperiodic components under EC and EO conditions may enhance diagnostic accuracy in the future.

Keywords. Electroencephalography, Dementia, Lewy Body, Parkinson, Alzheimer, Spectral analysis, Aperiodic, FOOOF

Journal Pre-proof

Journal Pre-proof

Introduction

Dementia is an umbrella term for conditions where there is decline in cognitive function, memory, and decision-making which has a significant functional impact on the lives of those affected (Centers for Disease Control and Prevention , 2019). Currently, there are approximately 58 million people worldwide with dementia, and it is projected to increase to 153 million by 2050 (Nichols et al., 2022). Various neurodegenerative disorders lead to the development of dementia, with Alzheimer's disease (AD) being the most common, accounting for ~70 % of cases. The second most prevalent type is Lewy body dementia (LBD), which encompasses Parkinson's disease dementia (PDD) and dementia with Lewy bodies (DLB). Although PDD and DLB share many clinical and morphological features, DLB is diagnosed when dementia precedes or coexists with motor parkinsonism (McKeith et al, 2017).

The neuropathology of dementia subtypes is associated with distinct behavioural and cognitive symptoms. AD features cerebral atrophy, beta-amyloid (Aβ) plaques and neurofibrillary (tau) tangles (NFTs). LBDs, including DLB and PDD, are marked by α-synuclein accumulation (Lewy Bodies), affecting attention and cognition, and causing visual hallucinations, parkinsonism, and REM sleep behaviour disorder (McKeith et al., 2017). The exact role of amyloid, tau and α-synuclein in these conditions are complex, with many cases showing mixed pathologies (Kapasi et al., 2017; Toledo et al., 2023), which impacts clinical progression and complicates diagnosis. Post-mortem findings reveal end-stage pathologies, not necessarily accounting for early disease initiators. Mild cognitive impairments can precede dementia by 10-15 years, yet such early impairments are sometimes reversible. Accurate and early diagnosis of patients is crucial to manage and alleviate symptoms and identify most promising interventions. Despite recent advances in blood-based biomarkers, it is apparent that there is no absolute diagnostic cut-off point for these, and identification of neurodegenerative disorders via functional measures, capable to capture subtle and early changes in neuronal communication, are essential.

Functional techniques, such as electroencephalography (EEG), are among the tools currently explored. EEG offers valuable diagnostic options due to its non-invasive, portable, and cost-

Journal Pre-proof

effective nature, allowing for direct measurement of neural activity with high temporal resolution. Despite its advantages, EEG is not routinely used in dementia clinics. This is primarily attributed to the lack of standardized EEG metrics independent of equipment and analysis techniques (Meghdadi et al., 2019). Research collectives and professional bodies have endeavoured to establish recommendations to achieve a degree of standardization within the field (Babiloni et al., 2020, 2021), yet guidelines still await widespread adaptation and consensus.

Quantitative EEG (qEEG) encompasses mathematical methods beyond visual inspection of recorded traces to decode neural activity (Livint Popa, et al, 2020), most commonly focussed on spectral patterns. Traditional qEEG applies Fast Fourier Transform (FFT) to convert the brain's discrete, time-domain signal into its frequency components. However, FFT operates under the assumption of signal stationarity and linearity, and thus overlooks the dynamic, non-linear and non-stationary nature of brain signals (Crouch et al., 2018). Alternatives such as autoregressive (AR) modelling enables transformation of EEG signals into the frequency domain based on a point-by-point approach that predicts future values based on previous data points. This process utilizes autocorrelation and regression to effectively model the signal and generate spectral information, incorporating an estimation error to account for the inherent unpredictability and noise within EEG recordings (Sommerlade et al., 2015). Hence, AR-generated spectra are smoother and offer a parametric perspective with enhanced spectral resolution (Crouch et al., 2018). Both FFT and AR can analyse the full spectrum or individual components of the signal, encompassing both its periodic and aperiodic elements.

As the field of qEEG is moving forward, other methods may offer valuable additional information. Over the past two decades, innovative methodologies have been proposed, among these are for example the evaluation of Sample Entropy (SaEn; Bruce et al., 2009), Ordinal pattern (OP) analysis (Ouyang et al., 2010), Fitting-Oscillations-&-One-Over-F (FOOOF) model (Donoghue et al., 2020) and assessment of Higuchi fractal dimensions (HDF; Higuchi, 1988; explored in Supplement C).

Journal Pre-proof

FOOOF is designed to distinguish oscillatory (periodic) and aperiodic (slope) properties of EEG signals. This approach deconstructs the EEG power spectrum into the aperiodic element, (background spectral density characterized by a 1/f-like distribution), and a sequence of Gaussian peaks that represent the oscillatory elements. Through this, FOOOF precisely estimates parameters (offset and exponent) and fits for the slope function of the aperiodic component alongside an examination of the periodic signals without background contribution. This approach has emerged as a promising approach to potentially differentiate between various forms of dementia (Wang et al., 2024) as it detects significant changes in the neural dynamics distinctive for specific disease states (Kopčanová et al., 2024). Although conventional methods for examining EEG signals, such as FFT and AR, have consistently observed hallmarks of dementia such as 'slowing' due to a shift in peak power (Baik et al., 2022; Dauwan et al., 2019; Musaeus et al., 2018; Peraza et al., 2018; Jelic et al., 2000) in individuals with cognitive impairments (Olde Dubbelink et al., 2013; Stoffers et al., 2007), however, no distinctive markers differentiating dementia subtypes have yet been identified.

In this study, we conducted a detailed comparative analysis to evaluate the effectiveness of various qEEG techniques in identifying and differentiating between dementia subtypes (AD, DLB and PDD). We analysed the spectral composition of EEGs from a dementia cohort via FFT and AR modelling and investigated parameters arising from the separation of periodic and aperiodic components of the AR EEG signal to determine if this enhances detection and distinction of the different dementia types.

Methods

Participants

Recordings of the Cognitive and Attentional Function in Lewy Body Disease (CATFieLD) study, which were previously published in other journals (see Schumacher et al., 2020; Stylianou et al., 2018), have been provided by the research group of Taylor et al. from Newcastle University, UK. Patients included in the study were diagnosed by experienced physicians according to specific criteria for DLB (McKeith et al., 2017), PDD (Emre et al.,

Journal Pre-proof

2007) and AD (McKhann et al., 2011) and were receiving appropriate medication for their clinical diagnoses. Patients were excluded if they presented any other neurological disorder or psychiatric condition. Neuropsychological tests, such as the Mini-Mental State Examination (MMSE) and the Cambridge Cognition Examination (CAMCOG) were collected for the patients included.

The CATFieLD dataset included 85 participants for EO and 82 for EC, diagnosed with Alzheimer's disease (AD), Parkinson's disease (PD), Dementia with Lewy bodies (DLB) or healthy control (Table 1). The number of patients included for EC/EO differed in the CTRL, AD and PDD groups, as the EEG recordings of one patient in each condition displayed a high number of noise and artifacts. Similarly, the frontal channels of one patient in the control group were excluded from all the analysis due to artefact issues.

Data acquisition

Resting-state EEG recordings were obtained from 128 electrodes placed on the scalp. These electrodes or channels were located according to the 10-5 international system, with a ground electrode placed on the right clavicle, and a reference for all derivations at Fz position. Recordings were performed during eyes open (EO) and eyes closed (EC) conditions for 2 minutes with a sampling rate of 1024Hz.

EEG data processing

A custom Matlab (Mathworks, version R2022b) script was used to read and select frontal (F3, F4), central (C3, C4), occipital (O1, O2) and temporal (T7 and T8) channels, included in this study. The electrode locations were deliberately chosen to facilitate the detection of signal alterations in brain regions that have been previously associated with or correlated to dementia (Latreille et al., 2016; Rodriguez et al., 1999). Then, 100-second episodes of artefact-free EEG recordings were identified and extracted from EO and EC conditions for each patient. Artifacts in the EEG signals were identified based on the presence of abnormal, high-amplitude aperiodic spikes, visually discernible within the EEG traces.

Journal Pre-proof

Fast Fourier Transform (FFT) spectral decomposition was performed using built-in MATLAB R2022b function (pwelch), which estimates the power spectral density (PSD) using overlapping segments. Each 4 second epoch was subjected to a Hamming window with a 50% overlap, and PSD was calculated for 0.5-48Hz, with 0.5Hz resolution.

Autoregressive (AR) spectral decomposition was performed using an in-house MATLAB R2022b script for each 4 sec epochs (Crouch et al., 2019). The spectral analyses were conducted from 0.5-48 Hz using an AR order of 256 points (1/4 of sample frequency) and a resolution of 0.5 Hz.

Spectral power analysis

After obtaining AR and FFT spectra, spectral power was calculated for each participant, separately for each condition and channel. Total FFT and AR spectra (0.5 - 45 Hz) were then converted to relative power by calculating the percentage of total power for FFT and by normalizing the AR power estimate of each individual frequency bin to the sum of all bins. Normalized spectra were divided into frequency ranges of interest and ultimately focussed on 4-15 Hz for each channel during EC and EO since the dominant frequency fell into this range when considering all groups. The variability of the dominant frequency was also pooled for each sample. The dominant frequency was defined as the average of the peak frequency of all 4 sec epochs, the dominant frequency variability was defined as its standard deviation.

Fitting-Oscillations-&-One-Over-F (FOOOF)

Parameterization of neural AR power spectra was conducted using the FOOOF algorithm (version 1.0.0; Donoghue et al., 2020) in Matlab (Mathworks, version R2022b). The parameters set in the model included a maximum number of peaks (5), minimum peak height (0.1), peak threshold (2.0) and peak width limits (1-10). The analysis encompassed the frequency spectrum of 1-45 Hz; the highest periodic peak of each epoch within the range of interest (4-15 Hz) were pooled for analysis. Statistical comparison of the mean periodic peak power, its frequency and frequency variability (SD of peak frequency) were conducted and

Journal Pre-proof

visually compared with results obtained from the traditional AR spectral analysis accounting for the full signal. In addition, FOOOF was employed to assess the aperiodic component of the EEG signal through its parameters, i.e. the offset representing the intercept of the aperiodic (non-oscillatory) component of the power spectrum; the exponent or the parameter that quantifies the slope of the aperiodic component; and the aperiodic fit (one phase decay of the non-oscillatory background activity) were evaluated at each channel for each group.

Statistical analysis

Standard statistical analyses were performed using GraphPad Prism 7 (GraphPad Software, La Jolla, California, USA). Significance was set to $p < 0.05$. Spectral comparisons between the dementia groups (AD, DLB and PDD) versus the control group were run via two-way ANOVAs followed by post hoc tests using Bonferroni correction for multiple comparisons. Secondly, groups were compared through estimation statistics (Ho et al., 2019). Estimation statistics can visualise the relative size of the mean (effect size) and the confidence interval (CI) and thus portray a better measure of magnitude and precision (see Supplement A). The estimation plots were created by the 'Shared Control Estimation stats and plot generator' (www.estimationstats.com), which compares groups by a two-sided permutation t-test. The effect size is calculated for each permutation P value by reshuffling 5000 times both the control and test group data. Results are represented as Cumming estimation plots and give the effect size as a bootstrap resampling for the 95% confidence interval (bias-corrected and accelerated). The P value reports the possibility of observing such an effect size if the null hypothesis of zero difference is true (Ho et al., 2019).

Dominant frequency, its variability, periodic peak power, periodic peak frequency, its variability and aperiodic parameters, exponent and offset values, were analysed using a mixed model design two-way ANOVA with Bonferroni post-hoc multiple comparisons test. In order to evaluate the distinctions in the aperiodic components of the signal between the different types of dementia and control groups, a one-phase exponential decay model was implemented on the aperiodic fit curves derived from each group (least square regression

Journal Pre-proof

and extra sum of squares F test). This tested whether the curves followed the same decay function or whether they differed significantly. Additionally, as a measure of quality control, the "goodness of fit" displayed as the coefficient of determination (R^2) is reported, and indicate a robust alignment between the predictive model and the empirical data (see Supplement B).

Results

Comparative examples of normalised EEG power spectra from C3 of AD, DLB and PDD patients are shown in Fig. 1 (FFT left, AR right), depicting the improved smoothing and noise reduction achieved by AR.

Statistical analysis comparing the spectral power of theta (4-8 Hz) and alpha (8-15 Hz) frequency bands derived from FFT and AR methods revealed general concordance between these procedures (Table 2), yet, FFT obtained a wider range of reliable significant differences, for example selectively affecting theta in PDD patients vs CTRL (EO). For alpha, group differences were limited to EC conditions, here, only FFT yielded a discrimination between AD vs CTRL.

As the primary objective of the present investigation was to optimise peak frequency analyses relevant for patients with cognitive impairments, we next opted to widen the frequency range of interest to incorporate the dominant frequency range (4-15 Hz) so that all relevant peaks of both dementia and healthy subjects were included (Table 3). For this range, FFT again detected far more significant differences between the study groups and CTRL compared to AR, but only during EO. It can be speculated that significances identified by both methods (highlighted in yellow in Tab. 3) are most robust and dominated by changes in the theta range (Table 2). Additional differences for the FFT analysis might be affected by false-positive results from noisy data, while excess averaging may lead to false negatives in AR spectra. However, only FFT identified multiple differences between PDD vs CTLR and AD (highlighted in green) during EO.

For AR, agreement was detected between eyes open and closed for the left central channel (C3) suggesting robust differences between DLB vs both CTRL and AD. All AR-based

significances suggested a clear pattern of lateralisation e.g in PDD at left frontal channel (EC) and in AD vs PDD at right central site (Table 3). These results were further corroborated and visualised through estimation statistics of AR spectral results (see Supplement A).

Based on AR spectra, the well-established slowing of the *dominant frequency* was robustly confirmed for all groups (except for the frontal pair in PDD), yet during EC only (Table 4; all ns for EO). The high significance of these changes and their consistency were also strikingly depicted in the corresponding estimation plots (Suppl. Fig. 1). Results for the *dominant frequency variability* are detailed in Table 5 and suggest a reduction particularly in all synuclein-related dementia groups (see also spectra Fig.1). This may underscore a reduced capacity for dynamic frequency modulation in synucleinopathies.

Analysis of *periodic and aperiodic components* of AR spectra was conducted next using the FOOOF approach, example fits and their components are given in Fig.2. Focusing first on the detection of peaks (corresponding to classic peak power data presented above), attributable to neural periodic oscillations within the targeted frequency range of 4-15 Hz, these were examined for their *power and frequency* characteristics. The comparative evaluation of *periodic peak power* derived from the FOOOF model revealed significant outcomes during EO for both synucleinopathy groups across most channels (Table 6). Findings that aligned with the AR spectral power analysis are denoted in yellow and showed a reliable overlap solely for DLB, facilitating the differentiation between DLB and control as well as AD (under both EO and EC conditions). Despite the absence of discernible differences for PDD in the AR spectral analysis, which includes both aperiodic and periodic signal components, the focused analysis on the periodic peak power unveiled significant changes. These changes were observed across frontal, central, and right occipital channels during EO conditions, with discriminators from AD at the central channels. Interestingly, a robust discrimination between AD and DLB was here also achieved during EC.

The analysis of *periodic peak frequency* (corresponding to dominant frequency analyses) elucidated significant distinctions across all examined groups, with notably consistent findings in both EO and EC conditions, as delineated in Table 7. Synucleinopathy groups exhibited

markedly reduced peak frequencies across all channels when compared to healthy controls, and differed from AD at central and occipital channels. The AD cohort demonstrated spectral alterations in the EO state at both occipital and temporal channels, as well as a single frontal channel (right frontal), and in the EC state at temporal channels along with one frontal channel (left frontal). A subtle differentiating factor between the synucleinopathies was observed only in EC at the occipital channels, where PDD presented a significantly slower peak compared to DLB. Crucially, classic dominant frequency analyses only revealed significant findings in the EC condition (Table 3), whereas a more pronounced array of alterations was observable in EO and EC when exclusively considering periodic signal components (Table 7).

Further, analysis of the *periodic peak frequency variability* largely agreed with AR peak variability analysis (Table 4), i.e. it identified changes predominantly in synucleinopathies vs CTRL and AD yet reported with more extensive differences (Table 8). Hence, this approach also delineated distinguishing features of synucleinopathies in comparison to AD in both EO and EC states, primarily at central (LBDs) and occipital channels (DLB).

Evaluation of the *aperiodic spectral parameters* delineated by the FOOOF model (Fig.2), specifically the *offset* (maximum) and the *exponent* (slope) offered a clear differentiation between control subjects and dementia cohorts (Table 9). This differentiation was only apparent during EC conditions, mirroring results obtained for the dominant frequency analysis (Table 3). Notably, across most channels, all groups exhibited significant variations in offset vs. CTRLS, with the exception of the frontal channels for AD and PDD cohorts. Conversely, alterations in the exponent in the PDD cohort were limited to central channels.

Further assessment of the decay function via *nonlinear fitting* of the aperiodic component (examples illustrated in Fig.3) yielded the most powerful differentiation among all groups from the study during both EO and EC, as delineated in Table 9. A comprehensive overview of key findings is summarised in Table 11.

Discussion

Spectral power analyses: Bands and peaks

Journal Pre-proof

Journal Pre-proof

This study evaluated spectral data within the 4-15 Hz range, encompassing both classic theta and alpha frequencies. We established the critical impact of the spectral range on standard EEG measures but also highlight that commonly used band borders may not allow detection of a genuine dominant / alpha peak in all conditions. The peak is generally reported to slow in individuals with cognitive impairments, hence shifting into the theta range (Anuradha et al., 2017; Olde Dubbelink et al., 2013; Stoffers et al., 2007). Conversely, in healthy individuals, the peak predominantly falls within the alpha range, especially during eyes open conditions (Schumacher et al., 2020; Markand, 1990). Traditional analyses based on theta and alpha power revealed significant disease-state dependent shifts specifically affecting the theta range, a phenomenon extensively documented (Baik et al., 2022; Dauwan et al., 2019; Musaeus et al., 2018; Peraza et al., 2018; Jelic et al., 2000). However, when spectral power for the combined 4-15 Hz range was compared, fewer distinctions emerged. To appropriately capture differences related to dominant peak analyses, we suggest the use of the wider range to enable robust peak inclusion across all groups, regardless of slowing. Other research groups have also proposed alternative frequency ranges that may offer superior analytical accuracy (Nuñez & Buño, 2021; Vinding et al., 2021; He et al., 2010). While oscillations in the 4-10 Hz range are crucial for memory and spatial navigation in healthy individuals (Buzsaki and Moser, 2013), adjustments in spectral analysis are needed to yield more accurate and comparable data to account for changes in patients with dementia.

Spectral FFT based methods have been extensively applied for the detection of brain diseases within research settings (Platt et al, 2011). However, their adoption in the routine clinical diagnosis of dementia still remains limited. EEG based diagnostics have faced criticism due to challenges related to reproducibility and reliability, a situation exacerbated by the lack of standardized parameters and protocols for clinical assessments (see Babiloni et al. 2020, 2021). Here, we identified FFT analysis as an effective spectral estimator for synucleinopathies within a clearly defined clinical cohort. This was particularly evident in distinguishing PDD vs control groups and AD patients during EO. Conversely, AR spectral data modelling may offer other advantages for diagnosing medical conditions, facilitating basic

research (Crouch et al., 2018, 2019), and pinpointing brain regions impacted by specific diseases (Ghafar et al., 2008). Yet, AR spectra have not yet been explored in-depth for their ability to discriminate between neurodegenerative conditions. Our study demonstrates the smoother and less noisy spectral appearance, and differentiation between DLB and control groups (CTRL), as well as DLB and AD, consistent with FFT based methods. Partial agreements between FFT and AR analyses were obtained for theta as well as over the wider 4-15 Hz range. Our data also suggest a potential for AR spectral analysis to reveal lateralization in DLB (4-15 Hz range). Furthermore, estimation statistics (see Supplement A) emphasised changes in spectral power during EC, particularly at the frontal pair and left central channels for PDD, suggesting that some alterations are not detected with traditional statistical methods. These findings underscore the value of utilizing effect sizes and their associated uncertainties through estimation methods (Claridge-Chang & Assam, 2016; Ho et al., 2019). Notably, neither FFT nor AR spectral analyses were able to robustly distinguish AD from healthy controls.

When isolating the periodic oscillations from the underlying signal (analysing peak power and frequency), more pronounced changes became apparent for both synucleinopathies during EO, with the DLB group exhibiting more significant alterations. This was more robustly detected compared to the conventional spectral power analysis. Additionally, focusing solely on periodic oscillations revealed alterations in the PDD group, mirroring findings from the traditional FFT spectral power analysis. These outcomes indicate that isolating periodic oscillations, rather than analysing the entire signal, can provide a more accurate method for identifying DLB and PDD. This approach also enhanced the differentiation of DLB from AD in EC conditions, a distinction that was less clear when using traditional spectral power analysis. Thus, periodic oscillations appear to be a more effective marker for identifying LBDs.

Dominant Frequency Slowing

All patient cohorts demonstrated significantly lower dominant frequencies (within 4-15 Hz) during EC. This substantiates the transition of dominant EEG peak power from the alpha to

Journal Pre-proof

Journal Pre-proof

the theta range in dementia patients (Barber et al., 2000; Bonanni et al., 2008; Briel et al., 1999; Micanovic & Pal, 2014; Peraza et al., 2018; Stylianou et al., 2018; van der Zande et al., 2018). Remarkably, when the analysis was adjusted to specifically detect the peak frequency of periodic components using FOOOF, a significant and consistent shift was confirmed, regardless of eyes being open or closed. The shift was reliable for AD and LBDs, but still more pronounced in patients with LBDs than AD, aligning with the above data and other studies that indicate a more substantial decrease in dominant frequency as a characteristic of synucleinopathies (Stylianou et al., 2018). This may be linked to a more severe cholinergic deficits present in LBD (Tiraboschi et al., 2002). Furthermore, periodic oscillations provided a distinction between the two types of synucleinopathies during EC at occipital channels, with PDD exhibiting a slower oscillation pattern than DLB. However, this observation necessitates further investigation, as the clinical manifestations of both forms of LBD can closely resemble each other at various stages of the disease (Schmitz et al., 2023).

The investigation of *dominant frequency variability* revealed largely matching insights using classical and FOOOF based methods, and estimation statistics. These approaches yielded complementary outcomes with synucleinopathies exhibiting lower variability than AD and CTRLS, except for a notable decrease in variability within the temporal region for AD when analysing the entire signal, encompassing both periodic and aperiodic components. This finding contrasts with Stylianou et al. (2018), who reported significantly increased variability in AD compared to controls within the theta-alpha frequency band. The discrepancies could be attributed to differences in the analytical methods and frequency ranges utilized. From a functional perspective, less variability of the peak frequency suggests a more rigid and inflexible network, in line with symptomatology seen in both DLB and PDD. Hence, periodic oscillatory activity may be more rigid in synucleinopathies than in AD, and despite AD and LBD both displaying a slowing pattern, patients with α-synucleinopathy might face greater challenges in adapting to cognitive demands, potentially leading to the cognitive slowdown commonly associated with LBD (Schumacher et al., 2019).

Journal Pre-proof

Aperiodic components

The study of the aperiodic component of EEG spectra offers novel revelations into the brain's physiological state and its functional integrity (Schaworonkow & Voytek, 2021; Wang et al., 2022). Here, alterations in aperiodic parameters, *offset* and *exponent*, observed in EC conditions, aligned closely with changes observed for the dominant frequency analysis of the signal. This suggests that aperiodic activity may play a role in the observed EEG slowing in dementia patients during EC, as detected through AR spectral analysis.

Variations in offset and exponent parameters were noted across all subtypes of dementia in EC conditions. Similar alterations have been identified in PD without dementia (Vinding et al., 2021), and are believed to be associated with the reduced dopamine levels found in LBD (Kim et al., 2022; Wiest et al., 2023). Interestingly, a previous study comparing AD patients to healthy individuals, while accounting for age, found no differences in offset and exponent evaluations (Kopčanová et al., 2023). This may suggest that the observed aperiodic component alterations in AD may primarily be driven by (accelerated?) age-related changes (Voytek et al., 2015; Donoghue et al., 2020). Additionally, Wang et al. (2022) discovered that early-stage PD patients on medication exhibited increased exponent and offset values compared to those off medication. Although these findings are not directly comparable with the results of our study, patients included here were also taking PD medication and displayed enhanced offset and exponent. This parameter thus requires careful consideration as an important confounder.

The *aperiodic fit* comparison revealed marked differences among all dementia subtypes as well as vs controls, indicating that non-rhythmic brain activity varies significantly across all groups. This approach was so robust that it discriminated regardless of eyes closed / open status. While normal aging may be associated with changes in the slope of aperiodic activity in older adults (Merkin et al., 2023; Voytek et al., 2015), recent research indicated that a steeper slope of aperiodic activity characterizes cognitively impaired elderly individuals (Aggarwal & Ray, 2023), aligning with our observations. Therefore, aging is likely a significant confounding factor, but the underlying mechanisms associated with dementia-specific

Journal Pre-proof

changes in aperiodic activity remain speculative. Proposed theories include a potential imbalance in the excitation-inhibition (E/I) ratio (Gao et al., 2017; Naskar et al., 2021), changes in brain morphology (Bédard et al., 2006), and neuronal physiological alterations (Bédard & Destexhe, 2009). These factors are closely related to each other and impact the brain's electrical activity of both periodic and aperiodic signals, as observed in neurodegenerative diseases such as AD, DLB and PDD.

Overall, our study investigated the utility of various quantitative EEG (qEEG) methods for analysing brain signals within the 4-15 Hz frequency range during both EO and EC conditions. Highlighting the role of frequency 'band' selection and partly non-aligned outcomes of AR spectra vs FFT analysis, results based on separating periodic and aperiodic signal components demonstrated superior capability in distinguishing between dementia subtypes. Although the influence of aging vs neurodegeneration on aperiodic activity warrants further investigation, our findings offer promising insights for enhancing the diagnostic precision of EEG to differentiate between AD, DLB, and PDD in the future.

Acknowledgement

This study is part of the academic postgraduate research of Masha Burelo, financed through the postgraduate fellowship program of the National Council of Science and Technology (CONACYT, by its Spanish acronym) of Mexico.

CRediT Author statement

Masha Burelo: writing, formal analysis, visualisation

Jack Bray: methodology, software, formal analysis, visualisation

Olga Gulka formal analysis, visualisation

Michael Firbank: investigation, data curation

John-Paul Taylor: investigation, writing (review), supervision, resources

Bettina Platt: conceptualisation, writing, supervision, resources, validation

Journal Pre-proof

References

Aggarwal, S., & Ray, S. (2023). Slope of the power spectral density flattens at low frequencies (<150 Hz) with healthy aging but also steepens at higher frequency (>200 Hz) in human electroencephalogram. *Cerebral Cortex Communications*, *4*(2). https://doi.org/10.1093/texcom/tgad011

Arezooji, D. M. (2020, July 19). *EEG-Fractal-Analysis*. Retrieved from Github: https://github.com/Dorsa-Arezooji/EEG-Fractal-Analysis

Babiloni C, Arakaki X, Azami H, Bennys K, Blinowska K, Bonanni L, Bujan A, Carrillo MC, Cichocki A, de Frutos-Lucas J, Del Percio C, Dubois B, Edelmayer R, Egan G, Epelbaum S, Escudero J, Evans A, Farina F, Fargo K, Fernández A, Ferri R, Frisoni G, Hampel H, Harrington MG, Jelic V, Jeong J, Jiang Y, Kaminski M, Kavcic V, Kilborn K, Kumar S, Lam A, Lim L, Lizio R, Lopez D, Lopez S, Lucey B, Maestú F, McGeown WJ, McKeith I, Moretti DV, Nobili F, Noce G, Olichney J, Onofrj M, Osorio R, Parra-Rodriguez M, Rajji T, Ritter P, Soricelli A, Stocchi F, Tarnanas I, Taylor JP, Teipel S, Tucci F, Valdes-Sosa M, Valdes-Sosa P, Weiergräber M, Yener G, Guntekin B. (2021) Measures of resting state EEG rhythms for clinical trials in Alzheimer's disease: Recommendations of an expert panel. *Alz Dement*. 2021 ;17(9):1528-1553. doi: 10.1002/alz.12311.

Babiloni, C., Barry, R. J., Başar, E., Blinowska, K. J., Cichocki, A., Drinkenburg, W. H. I. M., Klimesch, W., Knight, R. T., Lopes da Silva, F., Nunez, P., Oostenveld, R., Jeong, J., Pascual-Marqui, R., Valdes-Sosa, P., & Hallett, M. (2020). International Federation of Clinical Neurophysiology (IFCN) - EEG research workgroup: Recommendations on frequency and topographic analysis of resting state EEG rhythms. Part 1: Applications in clinical research studies. *Clin Neurophysiology*, *131*(1), 285–307.

https://doi.org/10.1016/j.clinph.2019.06.234

Baik, K., Jung, J. H., Jeong, S. H., Chung, S. J., Yoo, H. S., Lee, P. H., Sohn, Y. H., Kang, S. W., & Ye, B. S. (2022). Implication of EEG theta/alpha and theta/beta ratio in Alzheimer's and Lewy body disease. *Scientific Reports, 12*(1), 18706. https://doi.org/10.1038/s41598-022-21951-5

Journal Pre-proof

Barber, P. A., Varma, A. R., Lloyd, J. J., Haworth, B., Haworth, J. S. S., & Neary, D. (2000). The electroencephalogram in dementia with Lewy bodies. *Acta Neurologica Scandinavica*, *101*(1), 53–56. https://doi.org/10.1034/j.1600-0404.2000.00006.x

Bédard, C., & Destexhe, A. (2009). Macroscopic Models of Local Field Potentials and the Apparent 1/f Noise in Brain Activity. *Biophysical Journal*, *96*(7), 2589–2603. https://doi.org/10.1016/J.BPJ.2008.12.3951

Bédard, C., Kröger, H., & Destexhe, A. (2006). Does the 1/f Frequency Scaling of Brain Signals Reflect Self-Organized Critical States? *Physical Review Letters*, *97*(11), 118102. https://doi.org/10.1103/PhysRevLett.97.118102

Bonanni, L., Thomas, A., Tiraboschi, P., Perfetti, B., Varanese, S., & Onofrj, M. (2008). EEG comparisons in early Alzheimer's disease, dementia with Lewy bodies and Parkinson's disease with dementia patients with a 2-year follow-up. *Brain*, *131*(3), 690–705. https://doi.org/10.1093/brain/awm322

Briel, R. C. G., McKeith, I. G., Barker, W. A., Hewitt, Y., Perry, R. H., Ince, P. G., & Fairbairn, A. F. (1999). EEG findings in dementia with Lewy bodies and Alzheimer's disease. *Journal of Neurology, Neurosurgery & Psychiatry*, *66*(3), 401–403. https://doi.org/10.1136/jnnp.66.3.401

Buzsáki, G. & Moser EI (2013). Memory, navigation and theta rhythm in the hippocampal-entorhinal system. *Nat Neurosci*.; 16(2):130-8. doi: 10.1038/nn.3304.

Bruce, E. N., Bruce, M. C., & Vennelaganti, S. (2009). Sample entropy tracks changes in electroencephalogram power spectrum with sleep state and aging. *J Clin Neurophys*, *26*(4), 257–266. https://doi.org/10.1097/WNP.0b013e3181b2f1e3

Claridge-Chang, A., & Assam, P. N. (2016). Estimation statistics should replace significance testing. *Nature Methods*, *13*(2), 108–109. https://doi.org/10.1038/nmeth.3729

Crouch, B., Sommerlade, L., Veselcic, P., Riedel, G., Schelter, B., & Platt, B. (2018). Detection of time-, frequency- and direction-resolved communication within brain networks. *Scientific Reports*, *8*(1), 1825. https://doi.org/10.1038/s41598-018-19707-1

Journal Pre-proof

Crouch, B., Yeap, J. M., Pais, B., Riedel, G., & Platt, B. (2019). Of mice and motion: Behavioural-EEG phenotyping of Alzheimer's disease mouse models. *J Neurosci Methods*, *319*, 89–98. https://doi.org/10.1016/j.jneumeth.2018.06.028

Dauwan, M., Hoff, J. I., Vriens, E. M., Hillebrand, A., Stam, C. J., & Sommer, I. E. (2019). Aberrant resting-state oscillatory brain activity in Parkinson's disease patients with visual hallucinations: An MEG source-space study. *NeuroImage. Clinical, 22*, 101752. https://doi.org/10.1016/j.nicl.2019.101752

Donoghue, T., Haller, M., Peterson, E. J., Varma, P., Sebastian, P., Gao, R., Noto, T., Lara, A. H., Wallis, J. D., Knight, R. T., Shestyuk, A., & Voytek, B. (2020). Parameterizing neural power spectra into periodic and aperiodic components. *Nature Neurosci*, *23*(12), 1655–1665. https://doi.org/10.1038/s41593-020-00744-x

Emre, M., Aarsland, D., Brown, R., Burn, D. J., Duyckaerts, C., Mizuno, Y., Broe, G. A., Cummings, J., Dickson, D. W., Gauthier, S., Goldman, J., Goetz, C., Korczyn, A., Lees, A., Levy, R., Litvan, I., McKeith, I., Olanow, W., Poewe, W., … Dubois, B. (2007). Clinical diagnostic criteria for dementia associated with Parkinson's disease. *Movement Disorders*, *22*(12), 1689–1707. https://doi.org/10.1002/mds.21507

Gao, R., Peterson, E. J., & Voytek, B. (2017). Inferring synaptic excitation/inhibition balance from field potentials. *NeuroImage*, *158*, 70–78. https://doi.org/10.1016/J.NEUROIMAGE.2017.06.078

Ghafar, R., Hussain, A., Samad, S. A., & Tahir, N. M. (n.d.). Comparison Of FFT And AR Techniques For Scalp EEG Analysis. In *4th Kuala Lumpur International Conference on Biomedical Engineering 2008* (pp. 158–161). https://doi.org/10.1007/978-3-540-69139-6_43

He, B. J., Zempel, J. M., Snyder, A. Z., & Raichle, M. E. (2010). The temporal structures and functional significance of scale-free brain activity. *Neuron, 66*(3), 353–369. https://doi.org/10.1016/j.neuron.2010.04.020

Journal Pre-proof

Higuchi, T. (1988). Approach to an irregular time series on the basis of the fractal theory. *Physica D: Nonlinear Phenomena, 31 (2),* 277-283. https://doi.org/10.1016/0167-2789(88)90081-4

Ho, J., Tumkaya, T., Aryal, S., Choi, H., & Claridge-Chang, A. (2019). Moving beyond P values: data analysis with estimation graphics. *Nature Methods*, *16*(7), 565–566. https://doi.org/10.1038/s41592-019-0470-3

Jelic, V., Johansson, S. E., Almkvist, O., Shigeta, M., Julin, P., Nordberg, A., Winblad, B., & Wahlund, L. O. (2000). Quantitative electroencephalography in mild cognitive impairment: longitudinal changes and possible prediction of Alzheimer's disease. *Neurobiol Aging, 21*(4), 533–540. https://doi.org/10.1016/s0197-4580(00)00153-6

Kapasi, A., DeCarli, C., & Schneider, J. A. (2017). Impact of multiple pathologies on the threshold for clinically overt dementia. *Acta Neuropathologica*, *134*(2), 171–186. https://doi.org/10.1007/s00401-017-1717-7

Kim, J., Lee, J., Kim, E., Choi, J. H., Rah, J. C., & Choi, J. W. (2022). Dopamine depletion can be predicted by the aperiodic component of subthalamic local field potentials. *Neurobiol Disease*, *168*, 105692. https://doi.org/10.1016/J.NBD.2022.105692

Kopčanová, M., Tait, L., Donoghue, T., Stothart, G., Smith, L., Sandoval, A. A. F., Davila-Perez, P., Buss, S., Shafi, M. M., Pascual-Leone, A., Fried, P. J., & Benwell, C. S. Y. (2023). Resting-state EEG signatures of Alzheimer's disease are driven by periodic but not aperiodic changes. *bioRxiv: the preprint server for biology*, 2023.06.11.544491. https://doi.org/10.1101/2023.06.11.544491

Latreille, V., Carrier, J., Gaudet-Fex, B., Rodrigues-Brazète, J., Panisset, M., Chouinard, S., Postuma, R. B., & Gagnon, J. F. (2016). Electroencephalographic prodromal markers of dementia across conscious states in Parkinson's disease. *Brain, 139*(Pt 4), 1189–1199. https://doi.org/10.1093/brain/aww018

Journal Pre-proof

Livint Popa, L., Dragos, H., Pantelemon, C., Verisezan Rosu, O., & Strilciuc, S. (2020). The Role of Quantitative EEG in the Diagnosis of Neuropsychiatric Disorders. *J Med and Life, 13*(1), 8–15. https://doi.org/10.25122/jml-2019-0085

Markand O. N. (1990). Alpha rhythms. *J Clin Neurophys 7*(2), 163–189. https://doi.org/10.1097/00004691-199004000-00003

McKeith, I. G., Boeve, B. F., Dickson, D. W., Halliday, G., Taylor, J.-P., Weintraub, D., Aarsland, D., Galvin, J., Attems, J., Ballard, C. G., Bayston, A., Beach, T. G., Blanc, F., Bohnen, N., Bonanni, L., Bras, J., Brundin, P., Burn, D., Chen-Plotkin, A., … Kosaka, K. (2017). Diagnosis and management of dementia with Lewy bodies. *Neurology*, *89*(1), 88–100. https://doi.org/10.1212/WNL.0000000000004058

McKhann, G. M., Knopman, D. S., Chertkow, H., Hyman, B. T., Jack, C. R., Kawas, C. H., Klunk, W. E., Koroshetz, W. J., Manly, J. J., Mayeux, R., Mohs, R. C., Morris, J. C., Rossor, M. N., Scheltens, P., Carrillo, M. C., Thies, B., Weintraub, S., & Phelps, C. H. (2011). The diagnosis of dementia due to Alzheimer's disease: Recommendations from the National Institute on Aging-Alzheimer's Association workgroups on diagnostic guidelines for Alzheimer's disease. *Alzheimer's & Dementia*, *7*(3), 263–269. https://doi.org/10.1016/j.jalz.2011.03.005

Meghdadi, A. H., Karic, M. S., & Berka, C. (2019). EEG analytics: benefits and challenges of data driven EEG biomarkers for neurodegenerative diseases. *2019 IEEE International Conference on Systems, Man and Cybernetics (SMC)*, 1280–1285. https://doi.org/10.1109/SMC.2019.8914065

Merkin, A., Sghirripa, S., Graetz, L., Smith, A. E., Hordacre, B., Harris, R., Pitcher, J., Semmler, J., Rogasch, N. C., & Goldsworthy, M. (2023). Do age-related differences in aperiodic neural activity explain differences in resting EEG alpha? *Neurobiol Aging*, *121*, 78–87. https://doi.org/10.1016/J.NEUROBIOLAGING.2022.09.003

Micanovic, C., & Pal, S. (2014). The diagnostic utility of EEG in early-onset dementia: a systematic review of the literature with narrative analysis. *J Neural Transmission*, *121*(1), 59–69. https://doi.org/10.1007/s00702-013-1070-5

Journal Pre-proof

Musaeus, C. S., Engedal, K., Høgh, P., Jelic, V., Mørup, M., Naik, M., Oeksengaard, A.-R., Snaedal, J., Wahlund, L.-O., Waldemar, G., & Andersen, B. B. (2018). EEG Theta Power Is an Early Marker of Cognitive Decline in Dementia due to Alzheimer's Disease. *J Alz Dis*, *64*(4), 1359–1371. https://doi.org/10.3233/JAD-180300

Naskar, A., Vattikonda, A., Deco, G., Roy, D., & Banerjee, A. (2021). Multiscale dynamic mean field (MDMF) model relates resting-state brain dynamics with local cortical excitatory–inhibitory neurotransmitter homeostasis. *Network Neuroscience*, 1–26. https://doi.org/10.1162/netn_a_00197

Nichols, E., Steinmetz, J. D., Vollset, S. E., Fukutaki, K., Chalek, J., Abd-Allah, F., Abdoli, A., Abualhasan, A., Abu-Gharbieh, E., Akram, T. T., Al Hamad, H., Alahdab, F., Alanezi, F. M., Alipour, V., Almustanyir, S., Amu, H., Ansari, I., Arabloo, J., Ashraf, T., … Vos, T. (2022). Estimation of the global prevalence of dementia in 2019 and forecasted prevalence in 2050: an analysis for the Global Burden of Disease Study 2019. *The Lancet Public Health*, *7*(2), e105–e125. https://doi.org/10.1016/S2468-2667(21)00249-8

Nuñez, A., & Buño, W. (2021). The Theta Rhythm of the Hippocampus: From Neuronal and Circuit Mechanisms to Behavior. *Frontiers Cell Neurosci*, *15*. https://doi.org/10.3389/fncel.2021.649262

Olde Dubbelink, K. T. E., Stoffers, D., Deijen, J. B., Twisk, J. W. R., Stam, C. J., & Berendse, H. W. (2013). Cognitive decline in Parkinson's disease is associated with slowing of resting-state brain activity: a longitudinal study. *Neurobiol Aging*, *34*(2), 408–418. https://doi.org/10.1016/J.NEUROBIOLAGING.2012.02.029

Ouyang, G., Dang, C., Richards, D. A., & Li, X. (2010). Ordinal pattern based similarity analysis for EEG recordings. *Clin Neurophysiol 121*(5), 694–703. https://doi.org/10.1016/j.clinph.2009.12.030

Peraza, L. R., Cromarty, R., Kobeleva, X., Firbank, M. J., Killen, A., Graziadio, S., Thomas, A. J., O'Brien, J. T., & Taylor, J.-P. (2018). Electroencephalographic derived network differences in Lewy body dementia compared to Alzheimer's disease patients. *Scientific Reports*, *8*(1), 4637. https://doi.org/10.1038/s41598-018-22984-5

Journal Pre-proof

Journal Pre-proof

Platt B, Welch A, Riedel G (2011). FDG-PET imaging, EEG and sleep phenotypes as translational biomarkers for research in Alzheimer's disease. *Biochem Soc Trans*. 39(4): 874-80. doi: 10.1042/BST0390874.

Rodriguez, G., Copello, F., Vitali, P., Perego, G., & Nobili, F. (1999). EEG spectral profile to stage Alzheimer's disease. *Clin Neurophysiol, 110*(10), 1831–1837. https://doi.org/10.1016/s1388-2457(99)00123-6

Schaworonkow, N., & Voytek, B. (2021). Longitudinal changes in aperiodic and periodic activity in electrophysiological recordings in the first seven months of life. *Devel Cognitive Neurosci*, *47*, 100895. https://doi.org/10.1016/J.DCN.2020.100895

Schmitz, M., Candelise, N., Canaslan, S., Altmeppen, H. C., Matschke, J., Glatzel, M., Younas, N., Zafar, S., Hermann, P., & Zerr, I. (2023). α-Synuclein conformers reveal link to clinical heterogeneity of α-synucleinopathies. *Trans Neurodegen, 12*(1), 12. https://doi.org/10.1186/s40035-023-00342-4

Schumacher, J., Peraza, L. R., Firbank, M., Thomas, A. J., Kaiser, M., Gallagher, P., O'Brien, J. T., Blamire, A. M., & Taylor, J. P. (2019). Dysfunctional brain dynamics and their origin in Lewy body dementia. *Brain 142*(6), 1767–1782. https://doi.org/10.1093/brain/awz069

Schumacher, J., Thomas, A. J., Peraza, L. R., Firbank, M., Cromarty, R., Hamilton, C. A., Donaghy, P. C., O'Brien, J. T., & Taylor, J.-P. (2020). EEG alpha reactivity and cholinergic system integrity in Lewy body dementia and Alzheimer's disease. *Alzheimer's Research & Therapy*, *12*(1), 46. https://doi.org/10.1186/s13195-020-00613-6

Sommerlade, L., Thiel, M., Mader, M., Mader, W., Timmer, J., Platt, B., & Schelter, B. (2015). Assessing the strength of directed influences among neural signals: An approach to noisy data. *J Neurosci Methods*, *239*, 47–64. https://doi.org/10.1016/J.JNEUMETH.2014.09.007

Stoffers, D., Bosboom, J. L. W., Deijen, J. B., Wolters, E. C., Berendse, H. W., & Stam, C. J. (2007). Slowing of oscillatory brain activity is a stable characteristic of Parkinson's disease without dementia. *Brain*, *130*(7), 1847–1860. https://doi.org/10.1093/brain/awm034

Stylianou, M., Murphy, N., Peraza, L. R., Graziadio, S., Cromarty, R., Killen, A., O' Brien, J. T., Thomas, A. J., LeBeau, F. E. N., & Taylor, J.-P. (2018). Quantitative

electroencephalography as a marker of cognitive fluctuations in dementia with Lewy bodies and an aid to differential diagnosis. *Clinical Neurophysiology*, *129*(6), 1209–1220. https://doi.org/10.1016/j.clinph.2018.03.013

Tiraboschi, P., Hansen, L. A., Alford, M., Merdes, A., Masliah, E., Thal, L. J., & Corey-Bloom, J. (2002). Early and widespread cholinergic losses differentiate dementia with Lewy bodies from Alzheimer disease. *Arch Gen Psychiatry,* *59*(10), 946–951. https://doi.org/10.1001/archpsyc.59.10.946

Toledo, J. B., Abdelnour, C., Weil, R. S., Ferreira, D., Rodriguez-Porcel, F., Pilotto, A., Wyman-Chick, K. A., Grothe, M. J., Kane, J. P. M., Taylor, A., Rongve, A., Scholz, S., Leverenz, J. B., Boeve, B. F., Aarsland, D., McKeith, I. G., Lewis, S., Leroi, I., Taylor, J. P., & ISTAART Lewy body dementias Trial Methods Working Group (2023). Dementia with Lewy bodies: Impact of co-pathologies and implications for clinical trial design. *Alzheimer's & Dementia* 19(1), 318–332. https://doi.org/10.1002/alz.12814

van der Zande, J. J., Gouw, A. A., van Steenoven, I., Scheltens, P., Stam, C. J., & Lemstra, A. W. (2018). EEG Characteristics of Dementia With Lewy Bodies, Alzheimer's Disease and Mixed Pathology. *Front Aging Neurosci*, *10*. https://doi.org/10.3389/fnagi.2018.00190

Vinding, M. C., Eriksson, A., Low, C. M. T., Waldthaler, J., Ferreira, D., Ingvar, M., Svenningsson, P., & Lundqvist, D. (2021). Different features of the cortical sensorimotor rhythms are uniquely linked to the severity of specific symptoms in Parkinson's disease. *MedRxiv*, 2021.06.27.21259592. https://doi.org/10.1101/2021.06.27.21259592

Voytek, B., Kramer, M. A., Case, J., Lepage, K. Q., Tempesta, Z. R., Knight, R. T., & Gazzaley, A. (2015). Age-Related Changes in 1/f Neural Electrophysiological Noise. *J Neurosci*, *35*(38), 13257–13265. https://doi.org/10.1523/JNEUROSCI.2332-14.2015

Wang, Z., Liu, A., Yu, J., Wang, P., Bi, Y., Xue, S., Zhang, J., Guo, H., & Zhang, W. (2024). The effect of aperiodic components in distinguishing Alzheimer's disease from frontotemporal dementia. *GeroScience*, 46(1), 751–768. https://doi.org/10.1007/s11357-023-01041-8

Journal Pre-proof

Journal Pre-proof

Wang, Z., Mo, Y., Sun, Y., Hu, K., Peng, C., Zhang, S., & Xue, S. (2022). Separating the aperiodic and periodic components of neural activity in Parkinson's disease. *Eur J Neurosci*, *56*(6), 4889–4900. https://doi.org/10.1111/ejn.15774

Wiest, C., Torrecillos, F., Pogosyan, A., Bange, M., Muthuraman, M., Groppa, S., Hulse, N., Hasegawa, H., Ashkan, K., Baig, F., Morgante, F., Pereira, E. A., Mallet, N., Magill, P. J., Brown, P., Sharott, A., & Tan, H. (2023). The aperiodic exponent of subthalamic field potentials reflects excitation/inhibition balance in Parkinsonism. *eLife*, *12*, e82467. https://doi.org/10.7554/eLife.82467

World Health Organization. (2023, March 15). *Dementia*. Retrieved from World Health Organization: https://www.who.int/news-room/fact-sheets/detail/dementia

Journal Pre-proof

Tables

	n		Age		Percentage of males		MMSE		CAMCOG	
Group	EO	EC	EO	EC	EO	EC	EO	EC	EO	EC
CTRL	21	20	75.67 ± 5.36	75.95 ± 5.34	66.67	65	29.14 ± 0.85	29.20 ± 0.89	96.52 ± 3.61	96.85 ± 3.73
AD	29	28	77.24 ± 7.46	76.11 ± 7.41	65.52	75	19.69 ± 4.42	20.18 ± 4.32	64.24 ± 16.07	66.04 ± 15.44
DLB*	22	22	74.77 ± 5.06	75.73 ± 5.67	95.45	86.36	23.05 ± 4.46	23.14 ± 4.41	76.91 ± 12	76.73 ± 12.11
PDD	13	12	72.85 ± 4.39	72.42 ± 4.29	100	100	23.85 ± 2.48	23.58 ± 2.39	77.15 ± 9.23	77 ± 9.62

Table 1. Summary of CATFieLD patients' demographic information. Values represent the mean ± SD of each group under eyes open (EO) and eyes closed (EC). PDD = Parkinson's Disease Dementia, DLB = Dementia with Lewy Bodies, AD = Alzheimer's Disease; MMSE = Mini Mental State Examination, CAMCOG = Cambridge Cognition Examination.

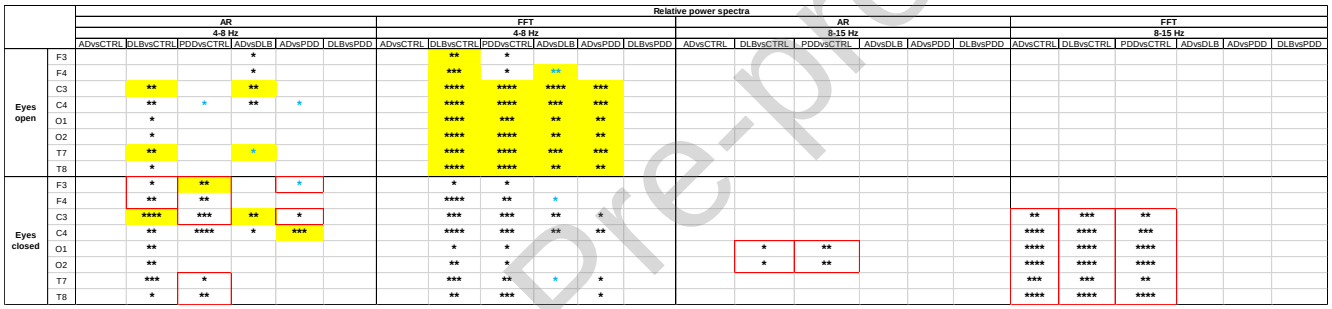

Table 2. AR vs FFT spectral power analysis for classic theta (4-8 Hz) and alpha (8-15 Hz) ranges using the autoregressive (AR) and Fast Fourier Transform (FFT) methods under eyes open and eyes closed conditions for eight channels. Groups of Alzheimer's disease (AD), Dementia with Lewy Bodies (DLB) and Parkinson's disease with dementia (PDD) were compared to each other and to the control group (CTRL). Agreement with the range of 4-15 Hz (Table 3) for both methods were found (yellow). Red outline of cells highlight changes detected only for EC. Potential lateralization is also pointed out (blue font colour). Data were analysed using two-way ANOVA followed by post hoc comparison using Bonferroni correction. The number of '*' corresponds to the significance of the statistical difference: $p < 0.05$, $p < 0.01$, $p < 0.001$. F3, F4 = Frontal left and right, C3, C4 = Central left and right, O1, O2 = Occipital left and right, T7, T8 = Temporal left and right.

Journal Pre-proof

		Relative AR power spectra						Relative FFT power spectra					
		4-15 Hz						4-15 Hz					
		ADvsCTRL	DLBvsCTRL	PDDvsCTRL	ADvsDLB	ADvsPDD	DLBvsPDD	ADvsCTRL	DLBvsCTRL	PDDvsCTRL	ADvsDLB	ADvsPDD	DLBvsPDD
Eyes open	F3								*				
	F4								**		*		
	C3		*		**				****	***	***	**	
	C4								***	**	**	*	
	O1								*	*	*	*	
	O2								**	**	*	*	
	T7		*		*				***	***	***	**	
	T8								**	**	**	*	
Eyes closed	F3			*									
	F4												
	C3		*		*								
	C4					*							
	O1												
	O2							*					
	T7												
	T8												

Table 3. **AR vs FFT spectral power analysis.** Spectral analysis of 4-15 Hz comparing autoregressive (AR) and Fast Fourier Transform (FFT) methods under eyes open and eyes closed conditions for eight channels. Groups of Alzheimer's disease (AD), Dementia with Lewy Bodies (DLB) and Parkinson's disease with dementia (PDD) were compared to each other and to the control group (CTRL). FFT and AR results exhibited some agreement (yellow). Green highlights significances between PDD and CTRL and PDD vs AD only detected with FFT. Red outline of cells highlights matching changes detected during EC and EO through AR. Data were analysed using two-way ANOVA followed by post hoc comparison using Bonferroni correction. The number of '*' corresponds to the significance of the statistical difference: $p < 0.05$, $p < 0.01$, $p < 0.001$. F3, F4 = Frontal left and right, C3, C4 = Central left and right, O1, O2 = Occipital left and right, T7, T8 = Temporal left and right.

		Dominant frequency					
		4-15 Hz					
		ADvsCTRL	DLBvsCTRL	PDDvsCTRL	ADvsDLB	ADvsPDD	DLBvsPDD
Eyes closed	F3	**	*				
	F4	*	**				
	C3	****	****	****			
	C4	****	****	****			
	O1	***	****	****			
	O2	**	****	****			
	T7	*****	****	****			
	T8	****	****	****			

Table 4. **Dominant frequency during eyes closed.** Comparison of peak frequency in eight channels was performed between 4-15 Hz. Alzheimer's disease (AD), Dementia with Lewy Bodies (DLB) and Parkinson's disease with dementia (PDD) compared to control were compared to each other and to the control group (CTRL). Data were analysed using mixed model two-way ANOVA followed by post hoc comparison using Bonferroni correction. Asterisks indicate p values, * = $p<0.05$, ** = $p<0.01$, *** = $p<0.001$. F3, F4 = Frontal left and right, C3, C4 = Central left and right, O1, O2 = Occipital left and right, T7, T8 = Temporal left and right.

Journal Pre-proof

		Dominant frequency variability					
		4-15 Hz					
		ADvsCTRL	DLBvsCTRL	PDDvsCTRL	ADvsDLB	ADvsPDD	DLBvsPDD
Eyes open	F3						
	F4		***	**			
	C3		*				
	C4		*				
	O1						
	O2		**	*			
	T7		***				
	T8	**	****	***			
Eyes closed	F3		*				
	F4		***	*			
	C3						
	C4				**	**	
	O1						
	O2				*	*	
	T7						
	T8						

Table 5. **Dominant frequency variability.** Comparison of dominant frequency variability at 4-15 Hz under eyes open and eyes closed conditions for eight channels. Alzheimer's disease (AD), Dementia with Lewy Bodies (DLB) and Parkinson's disease with dementia (PDD) groups were compared to each other and to the healthy group (CTRL). Agreement between both conditions (EO and EC) are indicated a with red outline of cells. Central and occipital channels (EC) were remarkable indicators of synucleinopathies vs AD during EC (yellow) and probable lateralization (blue asterisks) are also highlighted. Data were analysed using mixed model two-way ANOVA followed by post hoc comparison using Bonferroni correction. The number of '*' corresponds to the significance of the statistical difference: $p < 0.05$, $p < 0.01$, $p < 0.001$. F3, F4 = Frontal left and right, C3, C4 = Central left and right, O1, O2 = Occipital left and right, T7, T8 = Temporal left and right.

Journal Pre-proof

		Periodic peak power 4-15 Hz					
		ADvsCTRL	DLBvsCTRL	PDDvsCTRL	ADvsDLB	ADvsPDD	DLBvsPDD
Eyes open	F3		****	*	**		
	F4		****	*	**		
	C3		****	*	****	*	
	C4		***	*	****	*	
	O1		**		***		
	O2		**	*	***		
	T7		****		****		
	T8		**		***		
Eyes closed	F3				*		
	F4		*		*		
	C3				**		
	C4				**		
	O1						
	O2						
	T7				**		
	T8						

Table 6. **Periodic peak power analysis at 4-15 Hz.** Power comparison of the peaks based on AR spectra corrected for aperiodic component between AD, DLB and PDD vs. controls (CTRL) during eyes open and eyes closed is depicted. Matching of both EO and EC conditions are highlighted with red outline of cells. Agreement with AR spectral power comparison (yellow) of the signal was also found, and possible lateralization (blue asterisks) were observed. Statistically significant difference was determined by mixed model two-way ANOVA with Bonferroni post hoc multiple comparisons test. The number of '*' corresponds to the significance of the statistical difference: $p < 0.05$, $p < 0.01$, $p < 0.001$. F3, F4 = Frontal left and right, C3, C4 = Central left and right, O1, O2 = Occipital left and right, T7, T8 = Temporal left and right.

		Periodic peak frequency 4-15 Hz					
		ADvsCTRL	DLBvsCTRL	PDDvsCTRL	ADvsDLB	ADvsPDD	DLBvsPDD
Eyes open	F3		**	**			
	F4	**	****	***			
	C3		**	***		**	
	C4		***	****	*	***	
	O1	*	****	****	*	**	
	O2	**	****	****	*	*	
	T7	**	****	****			
	T8	**	****	****			
Eyes closed	F3	*	***	**			
	F4		***	***			
	C3		****	****	*	**	
	C4		****	****	**	***	
	O1		****	****	**	****	*
	O2		****	****	**	****	*
	T7	*	****	****	*	***	
	T8	**	****	****	**	**	

Table 7. **Periodic peak frequency analysis at 4-15 Hz.** Frequency comparison between AD, DLB and PDD vs. controls (CTRL) of the peak based on AR spectra corrected for aperiodic component during eyes open and eyes closed is illustrated. Matching of both EO and EC conditions are highlighted with red outline of cells. Agreement with dominant frequency

Journal Pre-proof

(yellow) of the signal was also found, and possible lateralization (blue asterisks) were observed. Data were analysed using mixed model two-way ANOVA followed by post hoc comparison using Bonferroni correction. Asterisks indicate p values, * = p<0.05, ** = p<0.01, *** = p<0.001. F3, F4 = Frontal left and right, C3, C4 = Central left and right, O1, O2 = Occipital left and right, T7, T8 = Temporal left and right.

		Periodic peak frequency variability					
		4-15 Hz					
		ADvsCTRL	DLBvsCTRL	PDDvsCTRL	ADvsDLB	ADvsPDD	DLBvsPDD
Eyes open	F3						
	F4		*	**		*	
	C3				***	**	
	C4			*	***	****	
	O1		***	**	****	**	
	O2		***		****		
	T7		**	*	***		
	T8		**		*		
Eyes closed	F3				**		
	F4				**		
	C3				*	*	
	C4				****	**	
	O1				*		
	O2				*	*	
	T7						
	T8					*	

Table 8. **Periodic peak frequency variability analysis at 4-15 Hz.** Comparison between AD, DLB and PDD vs. controls (CTRL) of the peak frequency variability based on AR spectra corrected for aperiodic component during eyes open and eyes closed is displayed. Matching of both EO and EC conditions are highlighted with red outline of cells. Agreement with dominant frequency variability (yellow) of the signal was also found, and possible lateralization (blue asterisks) were observed. Statistically significant difference was determined by mixed model two-way ANOVA with Bonferroni post hoc multiple comparisons test. The number of '*' corresponds to the significance of the statistical difference: $p < 0.05$, $p < 0.01$, $p < 0.001$. F3, F4 = Frontal left and right, C3, C4 = Central left and right, O1, O2 = Occipital left and right, T7, T8 = Temporal left and right.

Journal Pre-proof

Journal Pre-proof

		Offset					
		ADvsCTRL	DLBvsCTRL	PDDvsCTRL	ADvsPDD	ADvsDLB	PDDvsDLB
Eyes closed	F3		*				
	F4		***	*			
	C3	****	****	***			
	C4	***	****	*			
	O1	***	****	**		*	
	O2	**	****	**			
	T7	****	****	**			
	T8	*	***	***			
		Exponent					
		ADvsCTRL	DLBvsCTRL	PDDvsCTRL	ADvsPDD	ADvsDLB	PDDvsDLB
Eyes closed	F3						
	F4		**				
	C3	*	**	*			
	C4		**	*			
	O1	*	*				
	O2	*	*				
	T7	**	***				
	T8						

Table 9. **Aperiodic offset and exponent values for eyes closed condition.** Parameters of the aperiodic component of the signal estimated in the AR spectral range of 1-45 Hz were compared and displayed. Agreement of both parameters (offset and exponent) is highlighted in green. Statistical significance was determined by mixed model 2-way ANOVA with Bonferroni multiple comparisons test. * $p < 0.05$, ** $p < 0.01$, *** $p < 0.001$, **** $p < 0.0001$. F3, F4 = Frontal left and right, C3, C4 = Central left and right, O1, O2 = Occipital left and right, T7, T8 = Temporal left and right.

Journal Pre-proof

Journal Pre-proof

		Fit of aperiodic slope					
		ADvsCTRL	DLBvsCTRL	PDDvsCTRL	ADvsPDD	ADvsDLB	PDDvsDLB
Eyes open	F3	****	***	**	****	****	****
	F4	****	****	****		****	****
	C3	****	****		****	****	****
	C4	****	****	****	****	****	**
	O1	****	****	****	****	***	****
	O2	****	****	****	****	****	****
	T7	****	****			****	****
	T8	****	****	****		****	****
Eyes closed	F3	****	****	****	****	****	***
	F4	****	****	****	****	****	
	C3	****	****	****	****	****	***
	C4	****	****	****	****	****	****
	O1	****	****	****	****	****	****
	O2	****	****	****	****	****	****
	T7	****	****	****	****	****	****
	T8	****	****	****	****	****	

Table 10. **Aperiodic fit during eyes open and eyes closed**, estimated for the range of 1-45 Hz (least square regression and extra sum of squares F test)**.** Each dementia type differed significantly from controls and other conditions. Statistical significance * $p < 0.05$, ** $p < 0.01$, *** $p < 0.001$, **** $p < 0.0001$. F3, F4 = Frontal left and right, C3, C4 = Central left and right, O1, O2 = Occipital left and right, T7, T8 = Temporal left and right. CTRL = controls, AD = Alzheimer's disease, DLB = Dementia with Lewy bodies, PDD = Parkinson's disease dementia.

Journal Pre-proof

SUMMARY
Spectral Band and Peak Power Analyses
○ AR and FFT based theta power and dominant frequency analyses differentiated well between synucleinopathies vs. CTRLS and AD (EO and EC), yet AD vs CTRLS and PDD vs DLB did not differ. ○ FFT yielded the most widespread and strongest group significances for both the theta range and extended 4-15 Hz range. ○ Only FFT-based alpha band comparison during EC differentiated between all conditions vs. CTRLS ○ Lower dominant peak frequency variability was particularly apparent for synucleinopathies vs CTRLs and AD.
FOOOF based parameters
○ Periodic peak frequency discrimination was particularly successful between all groups but not robust for DLB vs PDD. ○ Periodic peak frequency variability also detected lower variability in synucleinopathies vs CTRLS but yielded more robust differences between synucleinopathies and AD. ○ Aperiodic parameters (offset and slope) offered excellent discrimination between all conditions and controls for both EO and EC. ○ The aperiodic fit comparison was the only approach that discriminated between all groups and under both EO and EC conditions.

Table 11. **Summary of main results during eyes closed (EC) and eyes open (EO) conditions**. CTRL = control group, AD = Alzheimer's disease, DLB = Dementia with Lewy bodies, PDD = Parkinson's disease dementia, F3, F4 = Frontal left and right, C3, C4 = Central left and right, O1, O2 = Occipital left and right, T7, T8 = Temporal left and right.

Journal Pre-proof

Figures and Legends

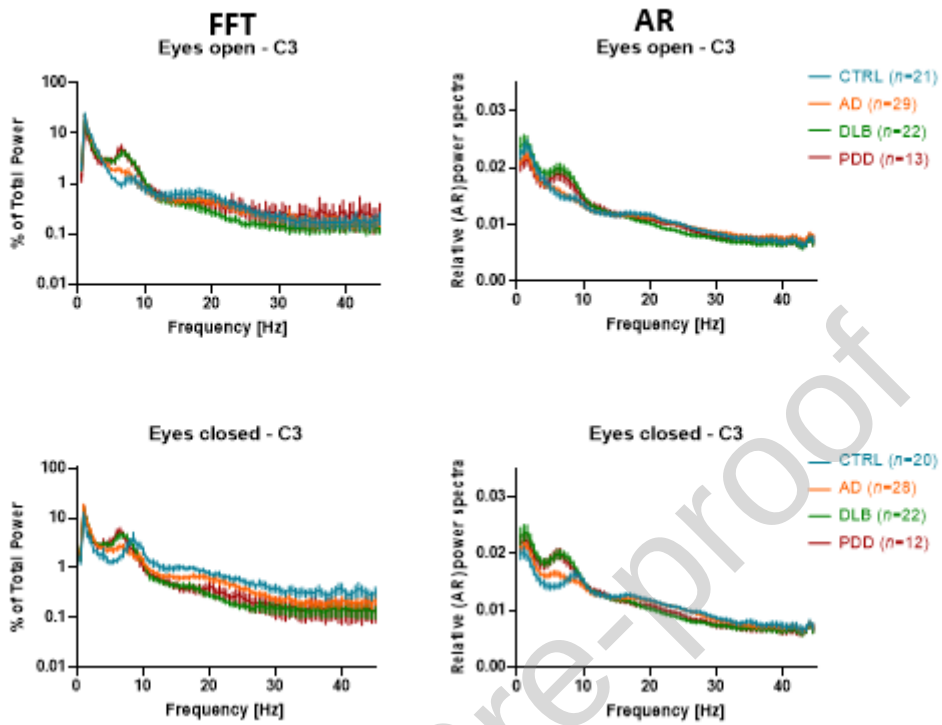

Figure 1. FFT (left) and AR (right) power spectra of the left central channel (C3). Normalised group (mean ± SEM) power spectra under eyes open and eyes closed conditions. CTRL = control group, AD = Alzheimer's disease, DLB = Dementia with Lewy bodies, PDD = Parkinson's disease dementia.

Journal Pre-proof

Journal Pre-proof

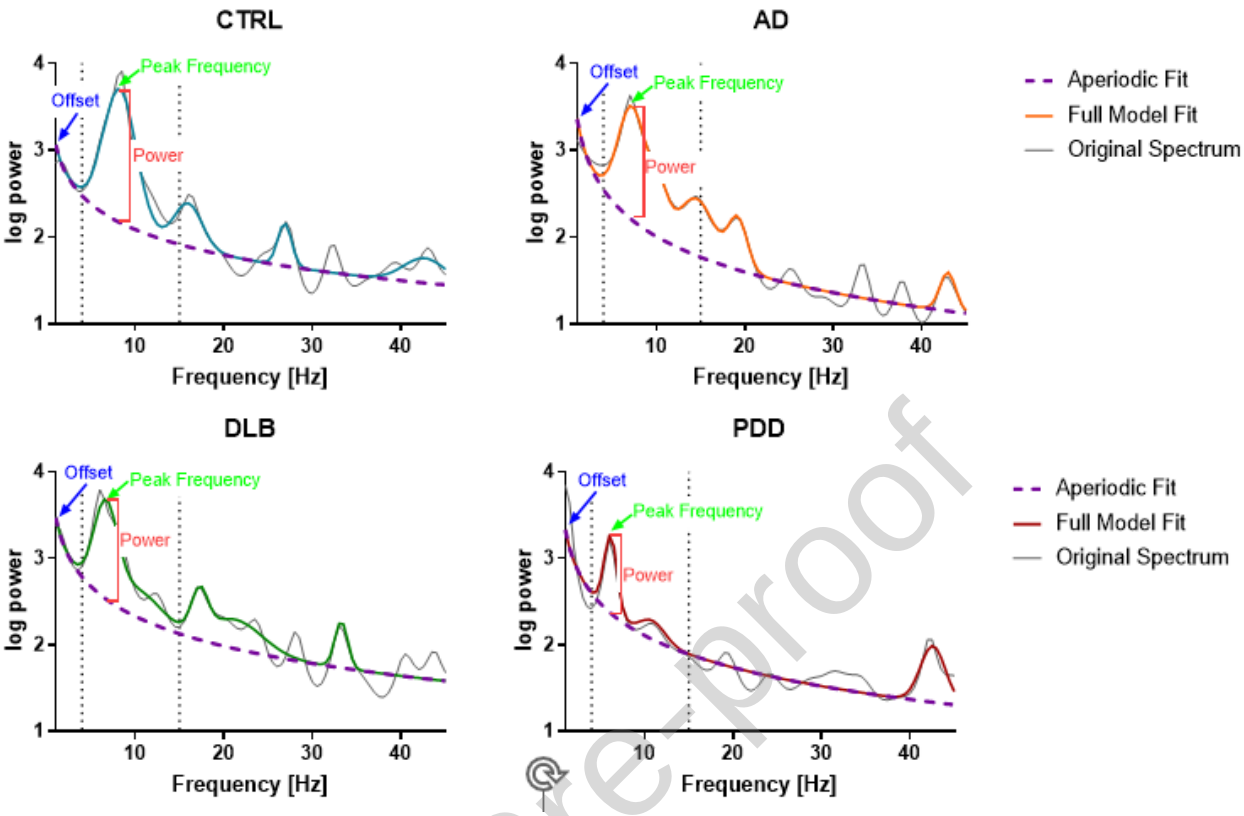

Figure 2. Exemplar FOOOF based modelling graphs of the right occipital channel (O2) from one representative patient per group (one epoch). Periodic peaks and exponential decay components are shown. CTRL = control group, AD = Alzheimer's disease, DLB = Dementia with Lewy bodies, PDD = Parkinson's disease dementia.

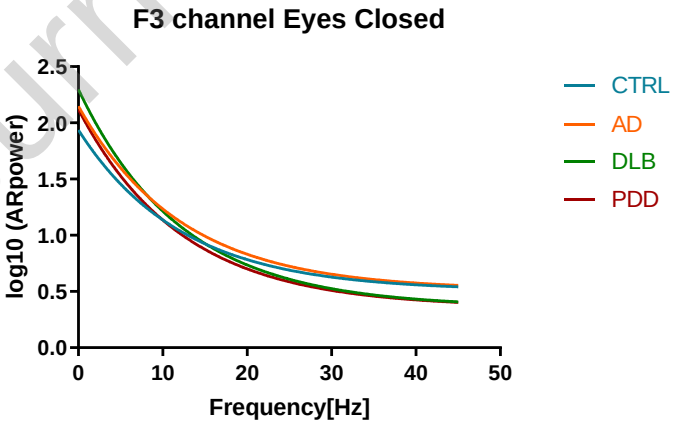

Figure 3. Example of the aperiodic fit of the aperiodic decay function. Graphic visualization for each group (AD, DLB, PDD and controls (CTRL)) for the left frontal channel during eyes closed. Error bars not included (for statistical results see Table 10).

Supplementary Material A: Estimation plots

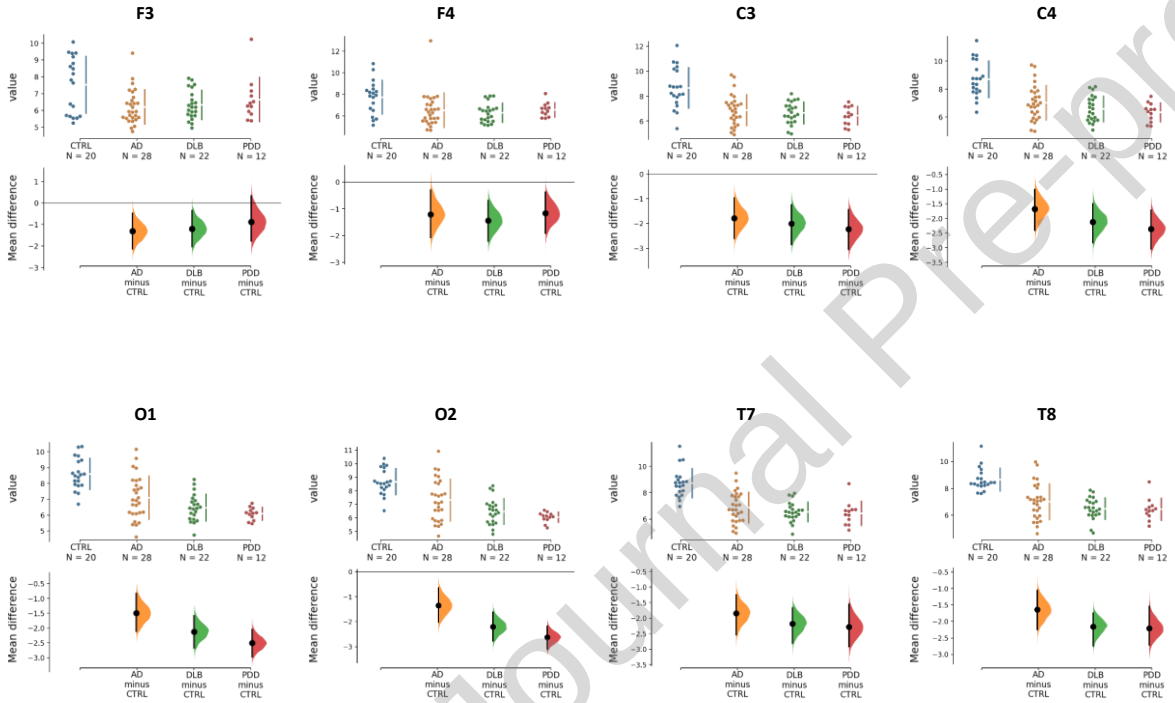

Suppl Figure 1. Estimation plots of the dominant frequency at 4-15 Hz during eyes closed condition. The mean difference for comparisons of all the disease groups (AD, DLB and PDD) versus the healthy control group (CTRL) are shown. These Cumming estimation plots represent mean differences based on nonparametric bootstrap resampling and the 95% confidence interval; each estimation depicts the plotted individual raw data on the upper graph; the effect size and distribution is visualised on the lower graph.

Journal Pre-proof

674

675

676

677

678

679

680

681

Journal Pre-proof

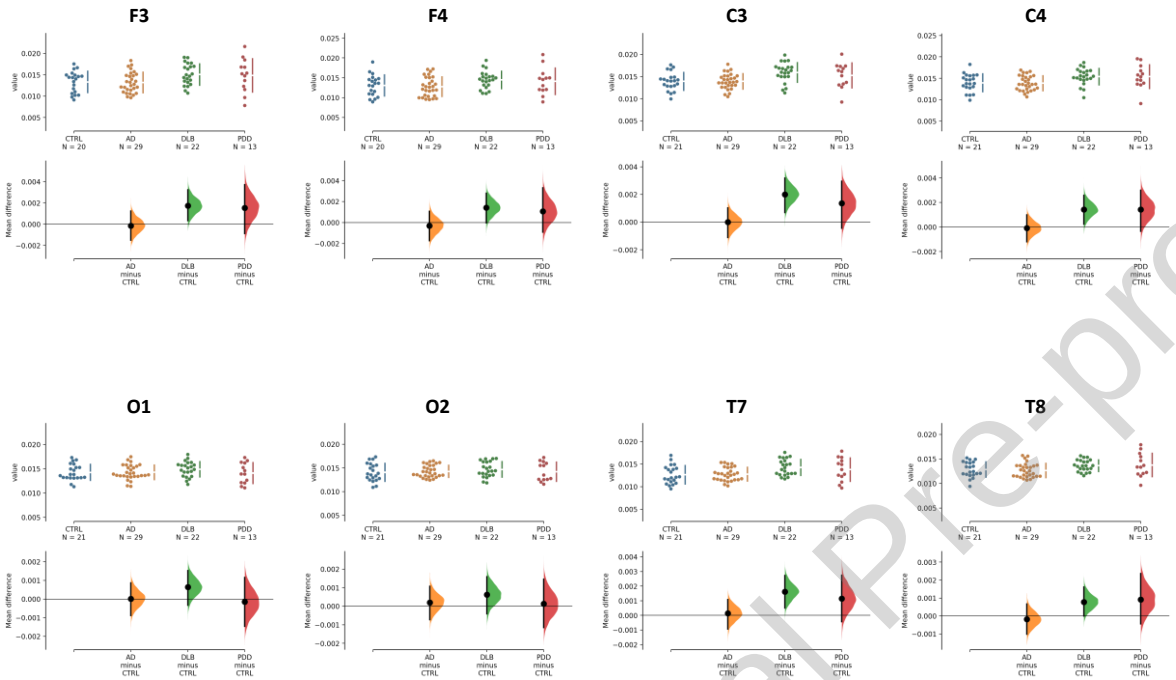

682

683 **Suppl Figure 2. Estimation plots of AR spectral power analysis (4-15 Hz) during eyes open**. Mean differences of the spectral
684 power comparing dementia groups (AD, DLB and PDD) versus the control group (CTRL). On each Cumming estimation plot, the
685 upper graph depicts the plotted individual raw data, while the lower graph summarises the effect size and distribution (mean
686 differences based on nonparametric bootstrap resampling and the 95% confidence interval).

687

688

689

690

Journal Pre-proof

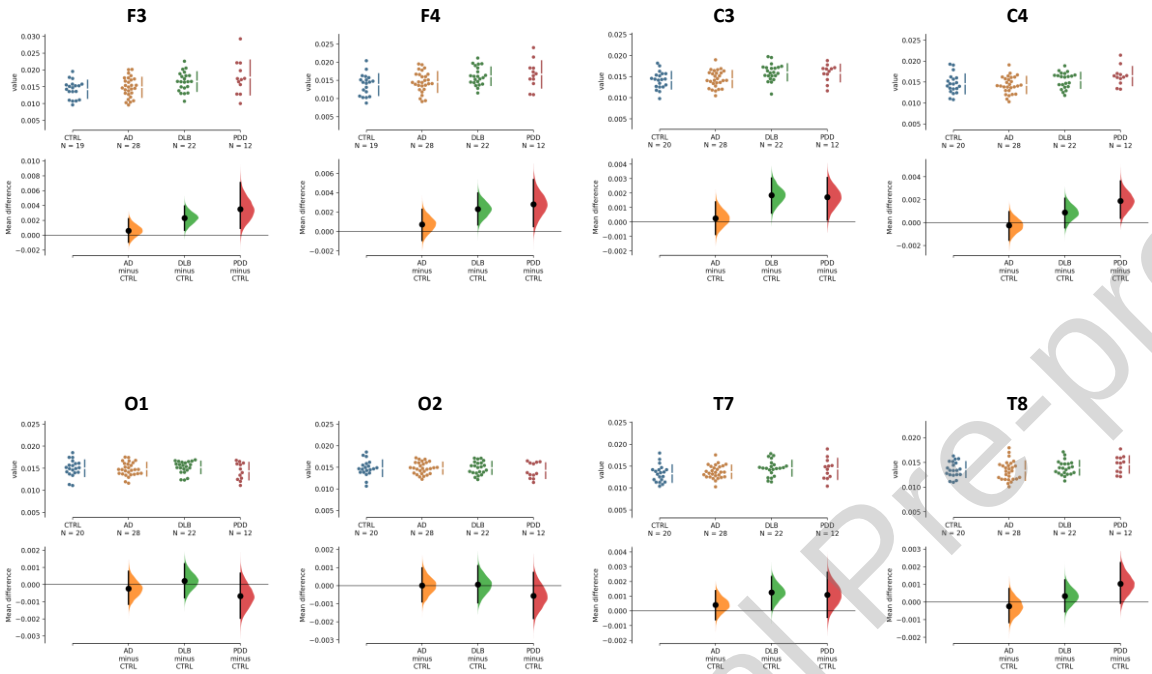

691

692 **Suppl Fig. 3. Estimation plots of AR spectral power analysis (4-15 Hz) during eyes closed**. Mean differences of the spectral
693 power comparing dementia groups (AD, DLB and PDD) versus the control group (CTRL). On each Cumming estimation plot, the
694 upper graph depicts the plotted individual raw data, while the lower graph summarises the effect size and distribution (mean
695 differences based on nonparametric bootstrap resampling and the 95% confidence interval).

696

Journal Pre-proof

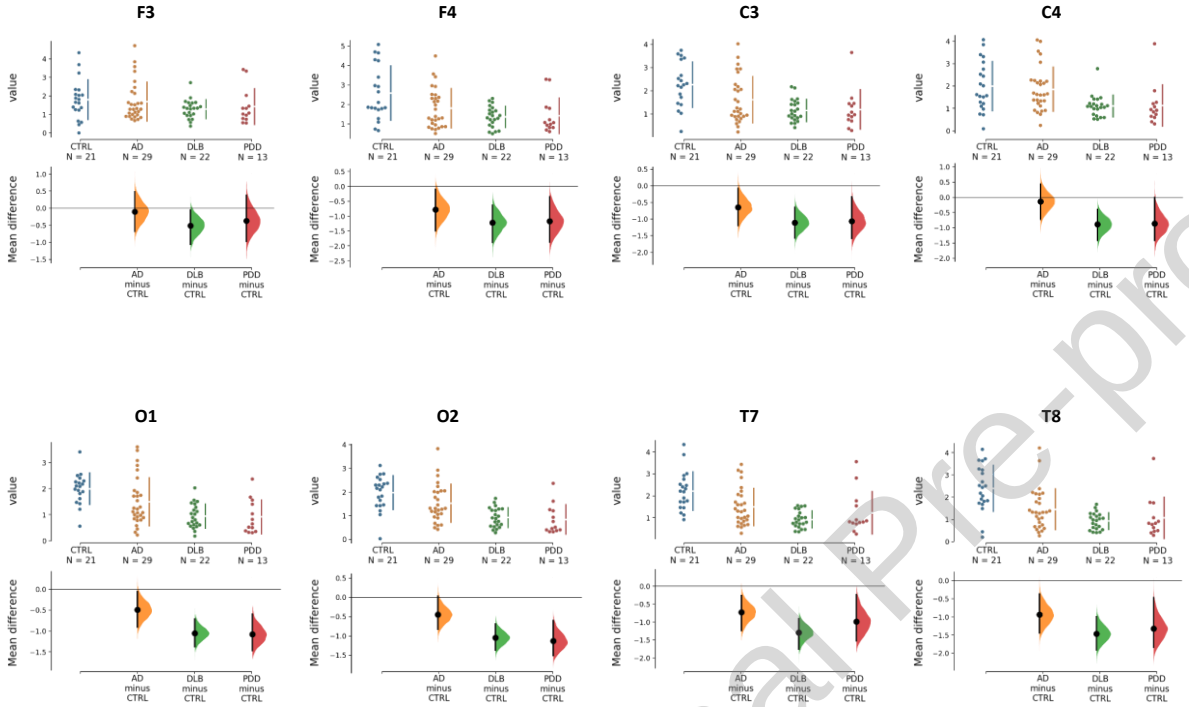

Suppl Fig. 4. Estimation plots of dominant frequency variability at 4-15 Hz during eyes closed. Alzheimer's disease (AD), Dementia with Lewy Bodies (DLB) and Parkinson's disease with dementia (PDD) groups versus the control group (CTRL) are shown in the Cumming estimation plots. Each one display the plotted individual raw data on the upper graph, the effect size and distribution is shown in the lower graph (mean differences based on nonparametric bootstrap resampling and the 95% confidence interval).

Journal Pre-proof

Supplementary Material B: Goodness of fit

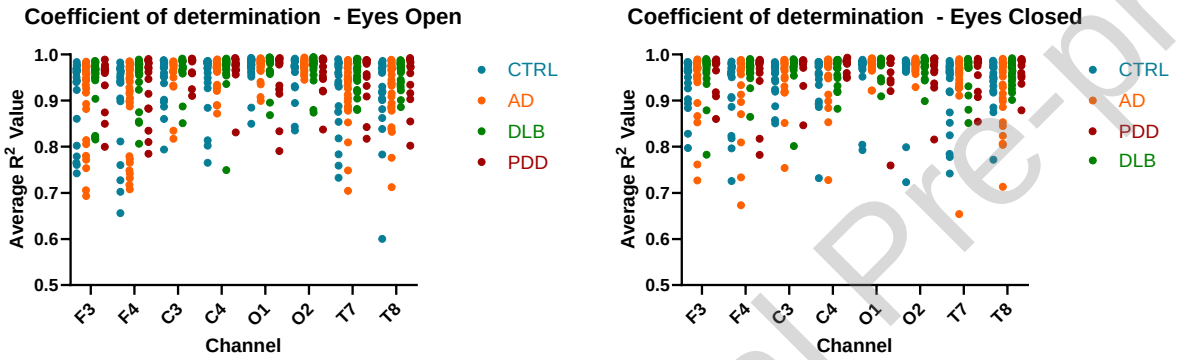

Suppl Fig. 5. Coefficient of determination (R^2). The R^2 metrics represent the explained variance of the model fit for each group, under eyes open and eyes closed conditions. CTRL = control group, AD = Alzheimer's disease, DLB = Dementia with Lewy bodies, PDD = Parkinson's disease dementia. F3, F4 = Frontal left and right, C3, C4 = Central left and right, O1, O2 = Occipital left and right, T7, T8 = Temporal left and right. No statistically significant difference was found as determined by mixed model two-way ANOVA with Bonferroni post hoc multiple comparisons test.

Journal Pre-proof

Supplementary Material C: Higuchi's fractal dimensions (HDF) analysis

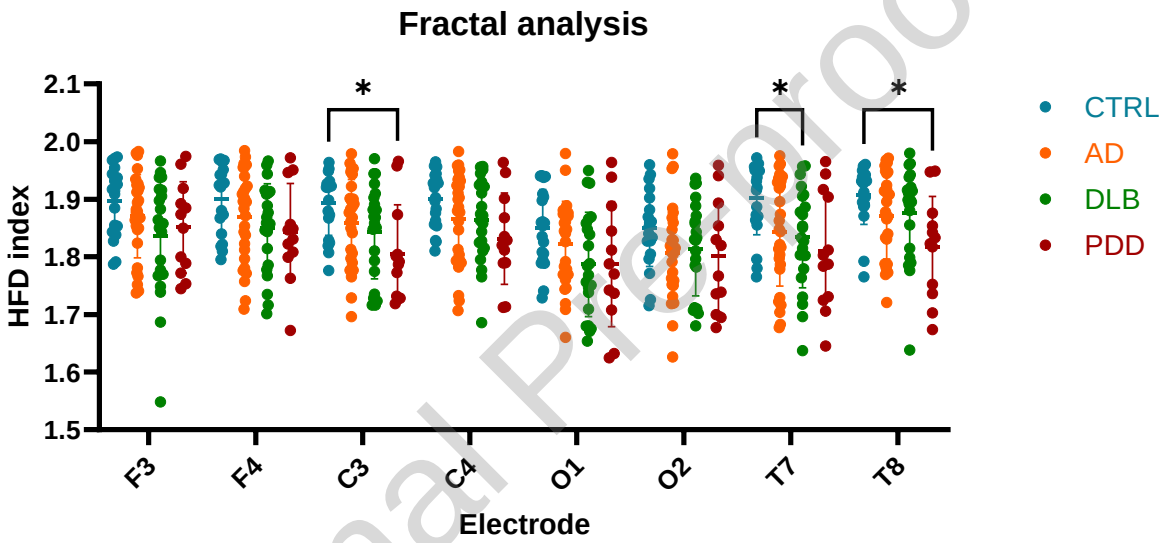

Suppl. Fig. 6. Higuchi's Fractal Dimension (HFD) index during eyes closed. Higuchi's fractal analysis was performed on 0-45 Hz of raw, unfiltered EEG signals with a script provided by Arezooji (2020). Comparison of HFD index of each dementia group to control is portrayed. Alzheimer's disease (AD), Dementia with Lewy bodies (DLB) and Parkinson's disease with dementia (PDD). Error bars represent standard deviation. Statistically significant difference was determined by mixed model analysis two-way ANOVA with Bonferroni post hoc multiple comparisons test. * $p < 0.05$, ** $p < 0.01$. F3, F4 = Frontal left and right, C3, C4 = Central left and right, O1, O2 = Occipital left and right, T7, T8 = Temporal left and right.

Journal Pre-proof

Declarations of interest:

None.

Journal Pre-proof

Tables

	n		Age		Percentage of males		MMSE		CAMCOG	
Group	EO	EC	EO	EC	EO	EC	EO	EC	EO	EC
CTRL	21	20	75.67 ± 5.36	75.95 ± 5.34	66.67	65	29.14 ± 0.85	29.20 ± 0.89	96.52 ± 3.61	96.85 ± 3.73
AD	29	28	77.24 ± 7.46	76.11 ± 7.41	65.52	75	19.69 ± 4.42	20.18 ± 4.32	64.24 ± 16.07	66.04 ± 15.44
DLB*	22	22	74.77 ± 5.06	75.73 ± 5.67	95.45	86.36	23.05 ± 4.46	23.14 ± 4.41	76.91 ± 12	76.73 ± 12.11
PDD	13	12	72.85 ± 4.39	72.42 ± 4.29	100	100	23.85 ± 2.48	23.58 ± 2.39	77.15 ± 9.23	77 ± 9.62

Table 1. Summary of CATFieLD patients' demographic information. Values represent the mean ± SD of each group under eyes open (EO) and eyes closed (EC). PDD = Parkinson's Disease Dementia, DLB = Dementia with Lewy Bodies, AD = Alzheimer's Disease; MMSE = Mini Mental State Examination, CAMCOG = Cambridge Cognition Examination.

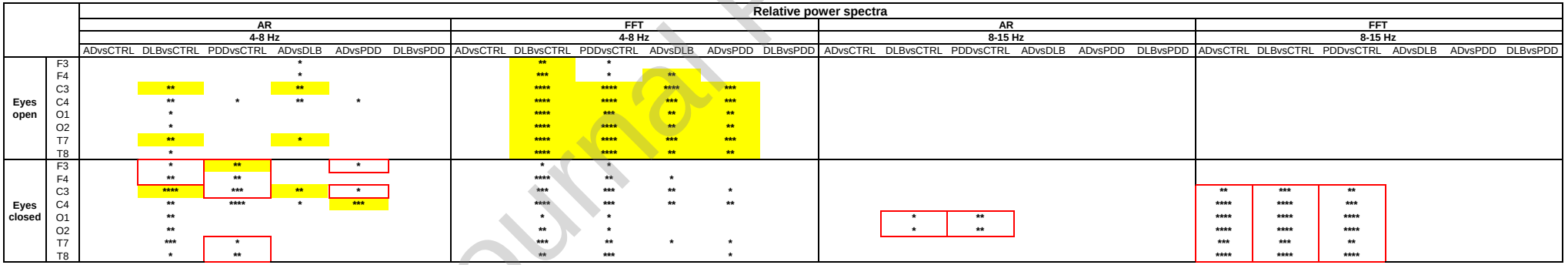

Table 2. AR vs FFT spectral power analysis for classic theta (4-8 Hz) and alpha (8-15 Hz) ranges using the autoregressive (AR) and Fast Fourier Transform (FFT) methods under eyes open and eyes closed conditions for eight channels. Groups of Alzheimer's disease (AD), Dementia with Lewy Bodies (DLB) and Parkinson's disease with dementia (PDD) were compared to each other and to the control group (CTRL). Agreement with the range of 4-15 Hz (Table 3) for both methods were found (yellow). Red outline of cells highlight changes detected only for EC. Potential lateralization is also pointed out (blue font colour). Data were analysed using two-way ANOVA followed by post hoc comparison using Bonferroni correction. The number of '*' corresponds to the significance of the statistical difference: $p < 0.05$, $p < 0.01$, $p < 0.001$. F3, F4 = Frontal left and right, C3, C4 = Central left and right, O1, O2 = Occipital left and right, T7, T8 = Temporal left and right.

Journal Pre-proof

		Relative AR power spectra						Relative FFT power spectra					
		4-15 Hz						4-15 Hz					
		ADvsCTRL	DLBvsCTRL	PDDvsCTRL	ADvsDLB	ADvsPDD	DLBvsPDD	ADvsCTRL	DLBvsCTRL	PDDvsCTRL	ADvsDLB	ADvsPDD	DLBvsPDD
Eyes open	F3								*				
	F4								**		*		
	C3		*		**				****	***	***	**	
	C4								***	**	**	*	
	O1								*	*	*	*	
	O2								**	**	*	*	
	T7		*		*				***	***	***	**	
	T8								**	**	**	*	
Eyes closed	F3			*									
	F4												
	C3		*		*								
	C4					*							
	O1												
	O2							*					
	T7												
	T8												

Table 3. **AR vs FFT spectral power analysis.** Spectral analysis of 4-15 Hz comparing autoregressive (AR) and Fast Fourier Transform (FFT) methods under eyes open and eyes closed conditions for eight channels. Groups of Alzheimer's disease (AD), Dementia with Lewy Bodies (DLB) and Parkinson's disease with dementia (PDD) were compared to each other and to the control group (CTRL). FFT and AR results exhibited some agreement (yellow). Green highlights significances between PDD and CTRL and PDD vs AD only detected with FFT. Red outline of cells highlights matching changes detected during EC and EO through AR. Data were analysed using two-way ANOVA followed by post hoc comparison using Bonferroni correction. The number of '*' corresponds to the significance of the statistical difference: $p < 0.05$, $p < 0.01$, $p < 0.001$. F3, F4 = Frontal left and right, C3, C4 = Central left and right, O1, O2 = Occipital left and right, T7, T8 = Temporal left and right.

		Dominant frequency					
		4-15 Hz					
		ADvsCTRL	DLBvsCTRL	PDDvsCTRL	ADvsDLB	ADvsPDD	DLBvsPDD
Eyes closed	F3	**	*				
	F4	*	**				
	C3	****	****	****			
	C4	****	****	****			
	O1	***	****	****			

Journal Pre-proof

	O2	**	****	****
	T7	*****	****	****
	T8	****	****	****

Table 4. **Dominant frequency during eyes closed.** Comparison of peak frequency in eight channels was performed between 4-15 Hz. Alzheimer's disease (AD), Dementia with Lewy Bodies (DLB) and Parkinson's disease with dementia (PDD) compared to control were compared to each other and to the control group (CTRL). Data were analysed using mixed model two-way ANOVA followed by post hoc comparison using Bonferroni correction. Asterisks indicate p values, * = p<0.05, ** = p<0.01, *** = p<0.001. F3, F4 = Frontal left and right, C3, C4 = Central left and right, O1, O2 = Occipital left and right, T7, T8 = Temporal left and right.

		Dominant frequency variability					
		4-15 Hz					
		ADvsCTRL	DLBvsCTRL	PDDvsCTRL	ADvsDLB	ADvsPDD	DLBvsPDD
Eyes open	F3						
	F4		***	**			
	C3		*				
	C4		*				
	O1						
	O2		**	*			
	T7		***				
	T8	**	****	***			
Eyes closed	F3		*				
	F4		***	*			
	C3						
	C4				**	**	
	O1						
	O2				*	*	
	T7						
	T8						

Table 5. **Dominant frequency variability.** Comparison of dominant frequency variability at 4-15 Hz under eyes open and eyes closed conditions for eight channels. Alzheimer's disease (AD), Dementia with Lewy Bodies (DLB) and Parkinson's disease with dementia (PDD) groups were compared to each other and to the healthy group (CTRL). Agreement between both conditions (EO and EC) are indicated a with red outline of cells. Central and occipital channels (EC) were remarkable indicators of synucleinopathies vs AD during EC (yellow) and probable lateralization (blue asterisks) are also highlighted. Data were analysed using mixed model two-way ANOVA followed by post hoc comparison using Bonferroni correction. The number of '*' corresponds to the significance of the statistical difference: p < 0.05, p < 0.01, p < 0.001. F3, F4 = Frontal left and right, C3, C4 = Central left and right, O1, O2 = Occipital left and right, T7, T8 = Temporal left and right.

Journal Pre-proof

768

769

		Periodic peak power					
		4-15 Hz					
		ADvsCTRL	DLBvsCTRL	PDDvsCTRL	ADvsDLB	ADvsPDD	DLBvsPDD
Eyes open	F3		****	*	**		
	F4		****	*	**		
	C3		****	*	****	*	
	C4		***	*	****	*	
	O1		**		***		
	O2		**	*	***		
	T7		****		****		
	T8		**		***		
Eyes closed	F3				*		
	F4		*		*		
	C3				**		
	C4				**		
	O1						
	O2						
	T7				**		
	T8						

770 **Table 6**. **Periodic peak power analysis at 4-15 Hz.** Power comparison of the peaks based on AR spectra corrected for aperiodic component
771 between AD, DLB and PDD vs. controls (CTRL) during eyes open and eyes closed is depicted. Matching of both EO and EC conditions are
772 highlighted with red outline of cells. Agreement with AR spectral power comparison (yellow) of the signal was also found, and possible
773 lateralization (blue asterisks) were observed. Statistically significant difference was determined by mixed model two-way ANOVA with Bonferroni
774 post hoc multiple comparisons test. The number of '*' corresponds to the significance of the statistical difference: $p < 0.05$, $p < 0.01$, $p < 0.001$.
775 F3, F4 = Frontal left and right, C3, C4 = Central left and right, O1, O2 = Occipital left and right, T7, T8 = Temporal left and right.
776
777

		Periodic peak frequency					
		4-15 Hz					
		ADvsCTRL	DLBvsCTRL	PDDvsCTRL	ADvsDLB	ADvsPDD	DLBvsPDD
Eyes open	F3		**	**			
	F4	**	****	***			
	C3		**	***		**	
	C4		***	****	*	***	
	O1	*	****	****	*	**	

Journal Pre-proof

	O2	**	****	****	*	*	
	T7	**	****	****			
	T8	**	****	****			
Eyes closed	F3	*	***	**			
	F4		***	***			
	C3		****	****	*	**	
	C4		****	****	**	***	
	O1		****	****	**	****	*
	O2		****	****	**	****	*
	T7	*	****	****	*	***	
	T8	**	****	****	**	**	

Table 7. **Periodic peak frequency analysis at 4-15 Hz.** Frequency comparison between AD, DLB and PDD vs. controls (CTRL) of the peak based on AR spectra corrected for aperiodic component during eyes open and eyes closed is illustrated. Matching of both EO and EC conditions are highlighted with red outline of cells. Agreement with dominant frequency (yellow) of the signal was also found, and possible lateralization (blue asterisks) were observed. Data were analysed using mixed model two-way ANOVA followed by post hoc comparison using Bonferroni correction. Asterisks indicate p values, * = p<0.05, ** = p<0.01, *** = p<0.001. F3, F4 = Frontal left and right, C3, C4 = Central left and right, O1, O2 = Occipital left and right, T7, T8 = Temporal left and right.

		Periodic peak frequency variability					
		4-15 Hz					
		ADvsCTRL	DLBvsCTRL	PDDvsCTRL	ADvsDLB	ADvsPDD	DLBvsPDD
Eyes open	F3						
	F4		*	**		*	
	C3				***	**	
	C4			*	***	****	
	O1		***	**	****	**	
	O2		***		****		
	T7		**	*	***		
	T8		**		*		
Eyes closed	F3				**		
	F4				**		
	C3				*	*	
	C4				****	**	
	O1				*		
	O2				*	*	
	T7						
	T8					*	

Journal Pre-proof

Table 8. **Periodic peak frequency variability analysis at 4-15 Hz.** Comparison between AD, DLB and PDD vs. controls (CTRL) of the peak frequency variability based on AR spectra corrected for aperiodic component during eyes open and eyes closed is displayed. Matching of both EO and EC conditions are highlighted with red outline of cells. Agreement with dominant frequency variability (yellow) of the signal was also found, and possible lateralization (blue asterisks) were observed. Statistically significant difference was determined by mixed model two-way ANOVA with Bonferroni post hoc multiple comparisons test. The number of '*' corresponds to the significance of the statistical difference: $p < 0.05$, $p < 0.01$, $p < 0.001$. F3, F4 = Frontal left and right, C3, C4 = Central left and right, O1, O2 = Occipital left and right, T7, T8 = Temporal left and right.

		Offset					
		ADvsCTRL	DLBvsCTRL	PDDvsCTRL	ADvsPDD	ADvsDLB	PDDvsDLB
Eyes closed	F3		*				
	F4		***	*			
	C3	****	****	***			
	C4	***	****	*			
	O1	***	****	**		*	
	O2	**	****	**			
	T7	****	****	**			
	T8	*	***	***			
		Exponent					
		ADvsCTRL	DLBvsCTRL	PDDvsCTRL	ADvsPDD	ADvsDLB	PDDvsDLB
Eyes closed	F3						
	F4		**				
	C3	*	**	*			
	C4		**	*			
	O1	*	*				
	O2	*	*				
	T7	**	***				
	T8						

Table 9. **Aperiodic offset and exponent values for eyes closed condition.** Parameters of the aperiodic component of the signal estimated in the AR spectral range of 1-45 Hz were compared and displayed. Agreement of both parameters (offset and exponent) is highlighted in green. Statistical significance was determined by mixed model 2-way ANOVA with Bonferroni multiple comparisons test. * $p < 0.05$, ** $p < 0.01$, *** $p < 0.001$, **** $p < 0.0001$. F3, F4 = Frontal left and right, C3, C4 = Central left and right, O1, O2 = Occipital left and right, T7, T8 = Temporal left and right.

Journal Pre-proof

		Fit of aperiodic slope					
		ADvsCTRL	DLBvsCTRL	PDDvsCTRL	ADvsPDD	ADvsDLB	PDDvsDLB
Eyes open	F3	****	***	**	****	****	****
	F4	****	****	****		****	****
	C3	****	****		****	****	****
	C4	****	****	****	****	****	**
	O1	****	****	****	****	***	****
	O2	****	****	****	****	****	****
	T7	****	****			****	****
	T8	****	****	****		****	****
Eyes closed	F3	****	****	****	****	****	***
	F4	****	****	****	****	****	
	C3	****	****	****	****	****	***
	C4	****	****	****	****	****	****
	O1	****	****	****	****	****	****
	O2	****	****	****	****	****	****
	T7	****	****	****	****	****	****
	T8	****	****	****	****	****	

Table 10. **Aperiodic fit during eyes open and eyes closed**, estimated for the range of 1-45 Hz (least square regression and extra sum of squares F test)**.** Each dementia type differed significantly from controls and other conditions. Statistical significance * $p < 0.05$, ** $p < 0.01$, *** $p < 0.001$, **** $p < 0.0001$. F3, F4 = Frontal left and right, C3, C4 = Central left and right, O1, O2 = Occipital left and right, T7, T8 = Temporal left and right. CTRL = controls, AD = Alzheimer's disease, DLB = Dementia with Lewy bodies, PDD = Parkinson's disease dementia.

Journal Pre-proof

SUMMARY
Spectral Band and Peak Power Analyses
○ AR and FFT based theta power and dominant frequency analyses differentiated well between synucleinopathies vs. CTRLS and AD (EO and EC), yet AD vs CTRLS and PDD vs DLB did not differ. ○ FFT yielded the most widespread and strongest group significances for both the theta range and extended 4-15 Hz range. ○ Only FFT-based alpha band comparison during EC differentiated between all conditions vs. CTRLS ○ Lower dominant peak frequency variability was particularly apparent for synucleinopathies vs CTRLs and AD.
FOOOF based parameters
○ Periodic peak frequency discrimination was particularly successful between all groups but not robust for DLB vs PDD. ○ Periodic peak frequency variability also detected lower variability in synucleinopathies vs CTRLS but yielded more robust differences between synucleinopathies and AD. ○ Aperiodic parameters (offset and slope) offered excellent discrimination between all conditions and controls for both EO and EC. ○ The aperiodic fit comparison was the only approach that discriminated between all groups and under both EO and EC conditions.

Table 11. **Summary of main results during eyes closed (EC) and eyes open (EO) conditions**. CTRL = control group, AD = Alzheimer's disease, DLB = Dementia with Lewy bodies, PDD = Parkinson's disease dementia, F3, F4 = Frontal left and right, C3, C4 = Central left and right, O1, O2 = Occipital left and right, T7, T8 = Temporal left and right.

Journal Pre-proof

Figures and Legends

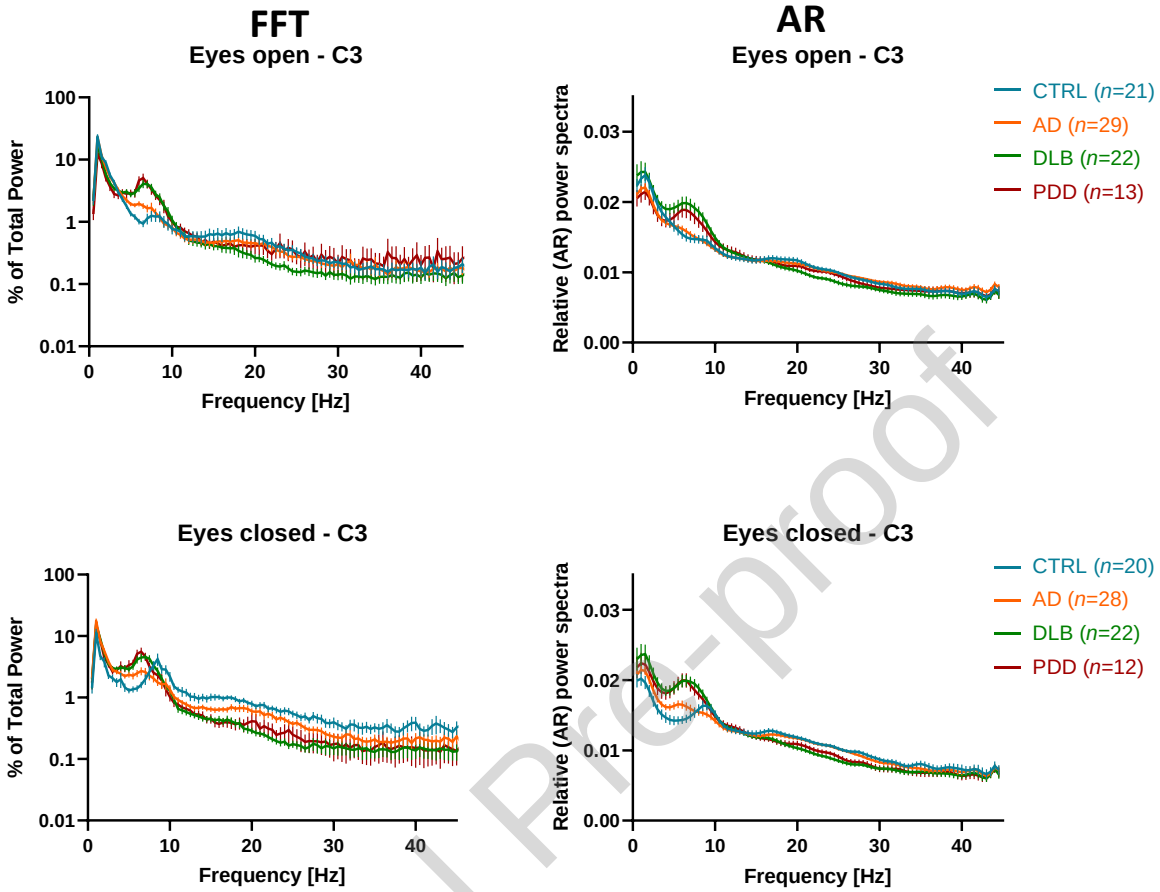

Figure 1. FFT (left) and AR (right) power spectra of the left central channel (C3). Normalised group (mean ± SEM) power spectra under eyes open and eyes closed conditions. CTRL = control group, AD = Alzheimer's disease, DLB = Dementia with Lewy bodies, PDD = Parkinson's disease dementia.

Journal Pre-proof

Journal Pre-proof

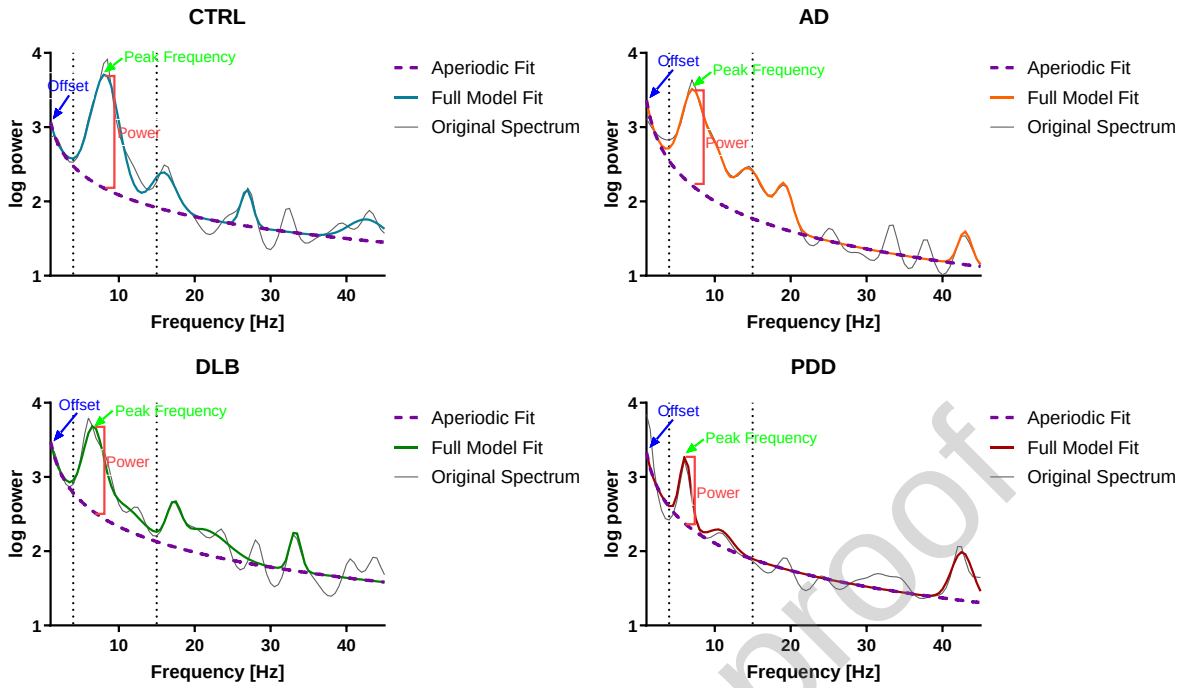

Figure 2. Exemplar FOOOF based modelling graphs of the right occipital channel (O2) from one representative patient per group (one epoch). Periodic peaks and exponential decay components are shown. CTRL = control group, AD = Alzheimer's disease, DLB = Dementia with Lewy bodies, PDD = Parkinson's disease dementia.

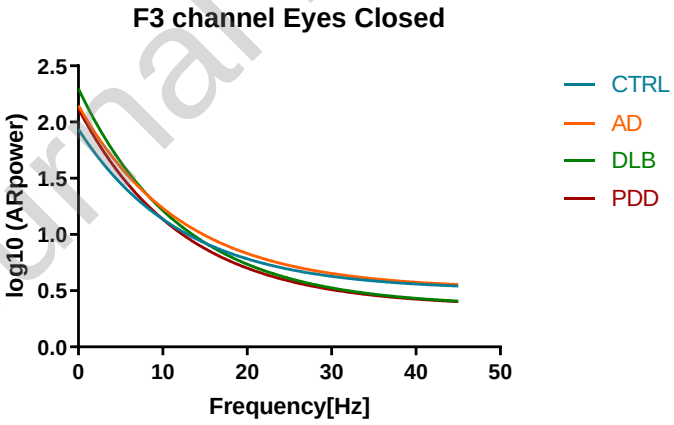

Figure 3. Example of the aperiodic fit of the aperiodic decay function. Graphic visualization for each group (AD, DLB, PDD and controls (CTRL)) for the left frontal channel during eyes closed. Error bars not included (for statistical results see Table 10).

Journal Pre-proof

Journal Pre-proof

Supplementary Material A: Estimation plots

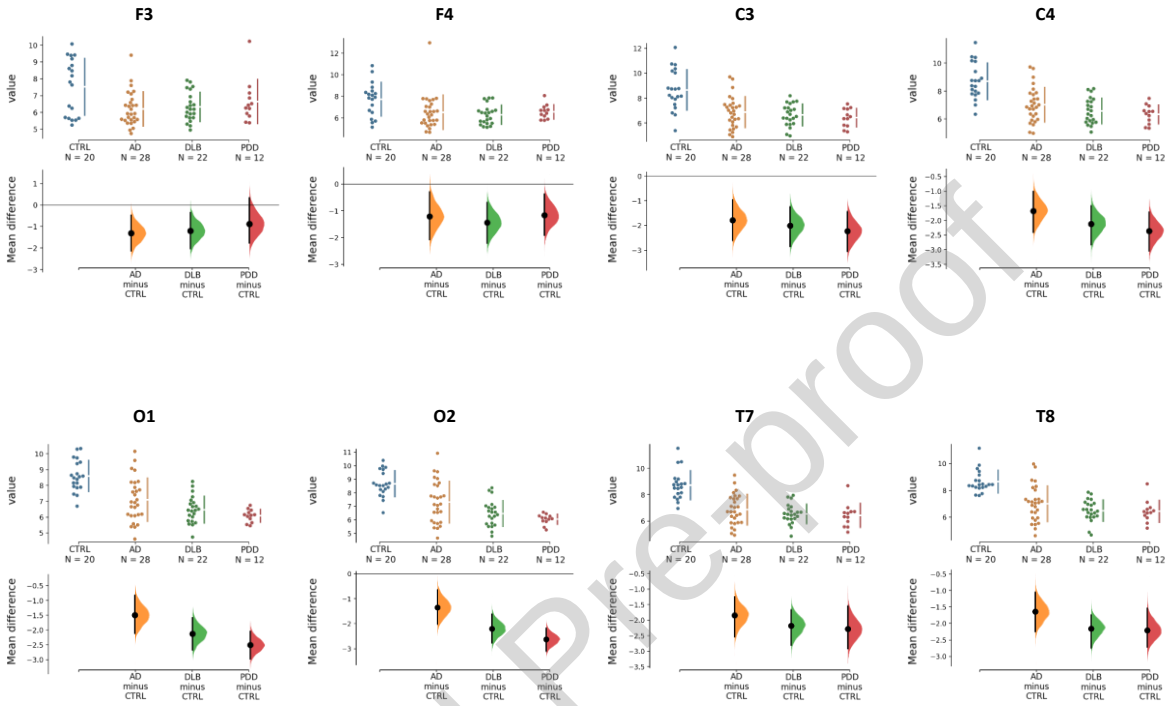

Suppl Figure 1. Estimation plots of the dominant frequency at 4-15 Hz during eyes closed condition. The mean difference for comparisons of all the disease groups (AD, DLB and PDD) versus the healthy control group (CTRL) are shown. These Cumming estimation plots represent mean differences based on nonparametric bootstrap resampling and the 95% confidence interval; each estimation depicts the plotted individual raw data on the upper graph; the effect size and distribution is visualised on the lower graph.

Journal Pre-proof

Journal Pre-proof

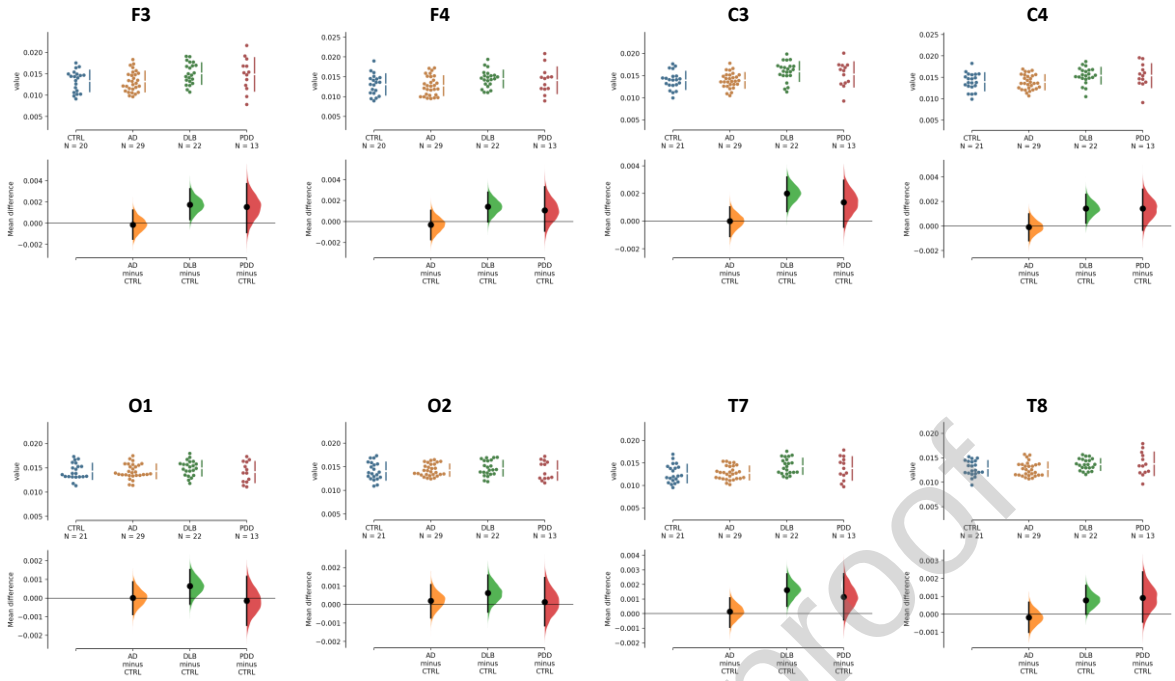

Suppl Figure 2. Estimation plots of AR spectral power analysis (4-15 Hz) during eyes open. Mean differences of the spectral power comparing dementia groups (AD, DLB and PDD) versus the control group (CTRL). On each Cumming estimation plot, the upper graph depicts the plotted individual raw data, while the lower graph summarises the effect size and distribution (mean differences based on nonparametric bootstrap resampling and the 95% confidence interval).

Journal Pre-proof

Journal Pre-proof

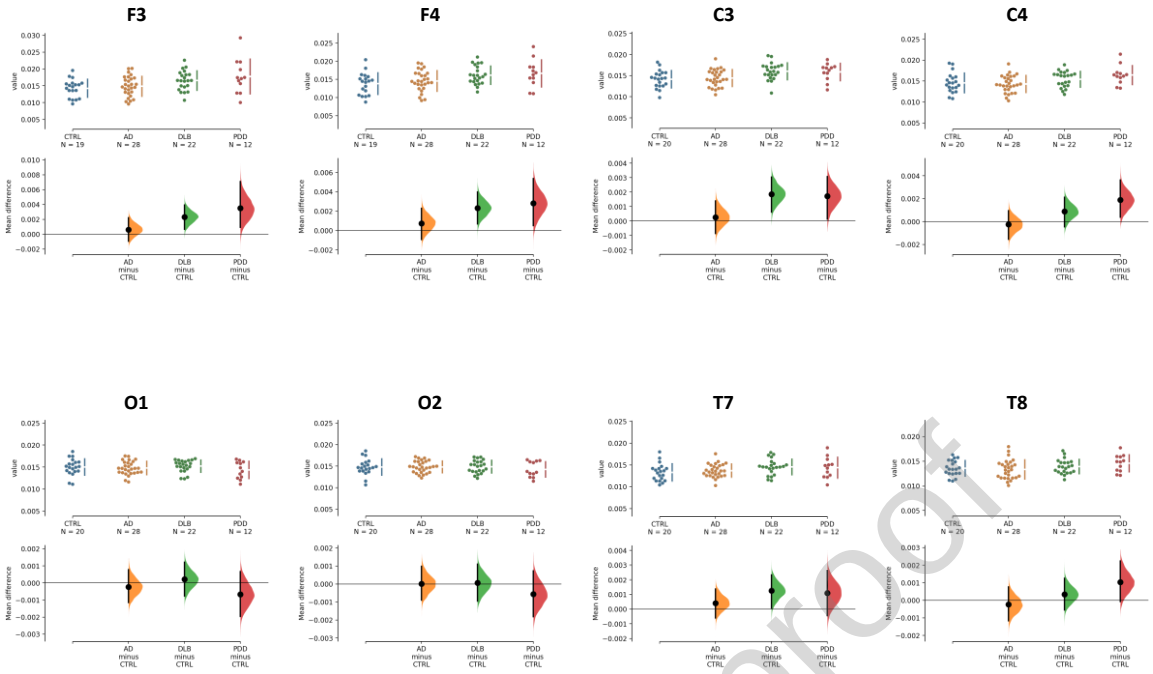

Suppl Fig. 3. Estimation plots of AR spectral power analysis (4-15 Hz) during eyes closed. Mean differences of the spectral power comparing dementia groups (AD, DLB and PDD) versus the control group (CTRL). On each Cumming estimation plot, the upper graph depicts the plotted individual raw data, while the lower graph summarises the effect size and distribution (mean differences based on nonparametric bootstrap resampling and the 95% confidence interval).

Journal Pre-proof

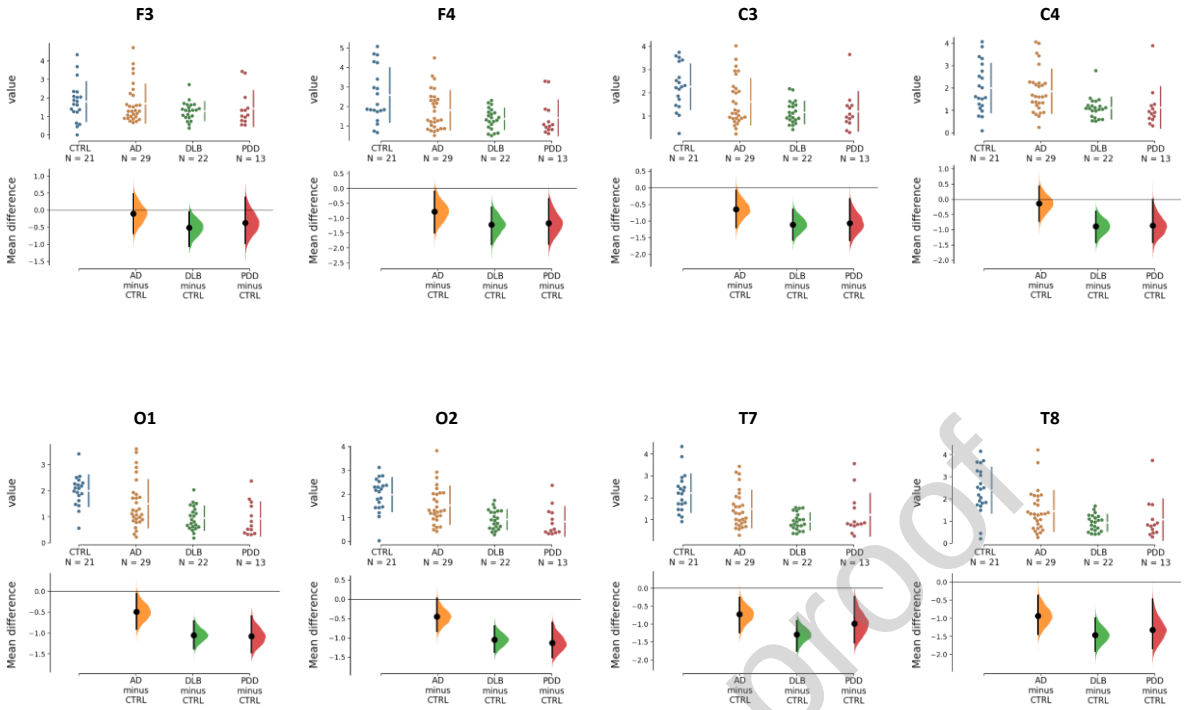

Suppl Fig. 4. Estimation plots of dominant frequency variability at 4-15 Hz during eyes closed. Alzheimer's disease (AD), Dementia with Lewy Bodies (DLB) and Parkinson's disease with dementia (PDD) groups versus the control group (CTRL) are shown in the Cumming estimation plots. Each one display the plotted individual raw data on the upper graph, the effect size and distribution is shown in the lower graph (mean differences based on nonparametric bootstrap resampling and the 95% confidence interval).

Journal Pre-proof

Supplementary Material B: Goodness of fit

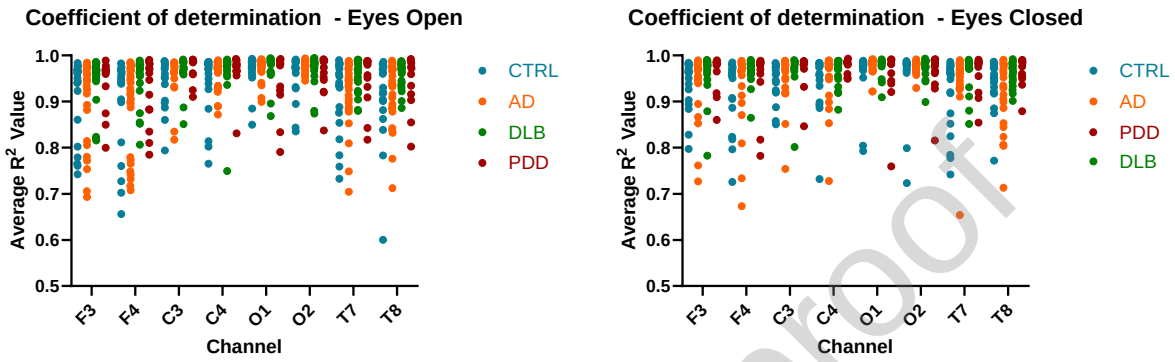

Suppl Fig. 5. Coefficient of determination (R^2). The R^2 metrics represent the explained variance of the model fit for each group, under eyes open and eyes closed conditions. CTRL = control group, AD = Alzheimer's disease, DLB = Dementia with Lewy bodies, PDD = Parkinson's disease dementia. F3, F4 = Frontal left and right, C3, C4 = Central left and right, O1, O2 = Occipital left and right, T7, T8 = Temporal left and right. No statistically significant difference was found as determined by mixed model two-way ANOVA with Bonferroni post hoc multiple comparisons test.

Journal Pre-proof

Journal Pre-proof

Supplementary Material C: Higuchi's fractal dimensions (HDF) analysis

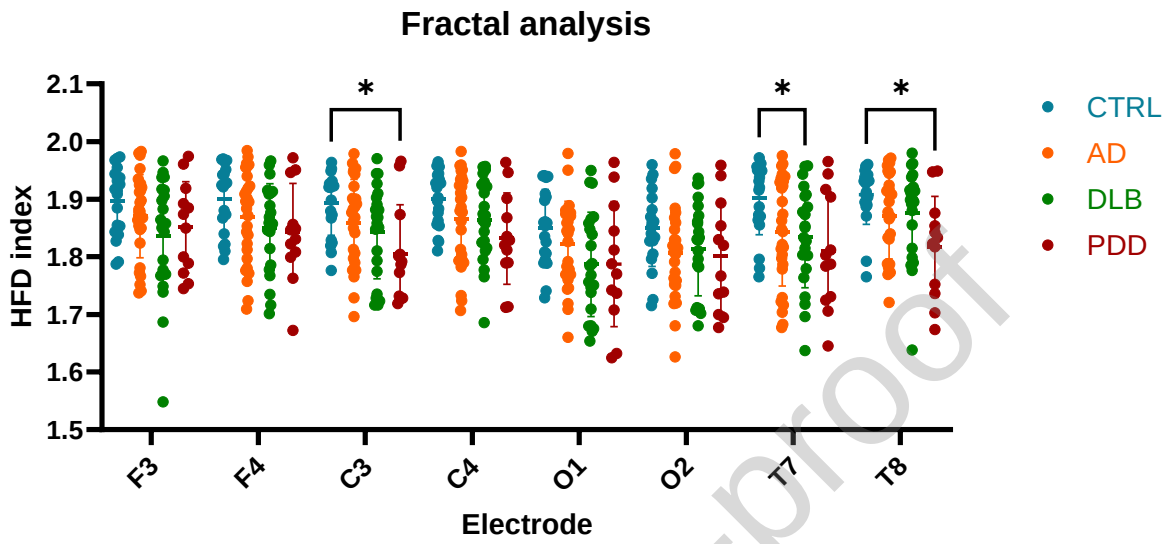

Suppl. Fig. 6. Higuchi's Fractal Dimension (HFD) index during eyes closed. Higuchi's fractal analysis was performed on 0-45 Hz of raw, unfiltered EEG signals with a script provided by Arezooji (2020). Comparison of HFD index of each dementia group to control is portrayed. Alzheimer's disease (AD), Dementia with Lewy bodies (DLB) and Parkinson's disease with dementia (PDD). Error bars represent standard deviation. Statistically significant difference was determined by mixed model analysis two-way ANOVA with Bonferroni post hoc multiple comparisons test. * $p < 0.05$, ** $p < 0.01$. F3, F4 = Frontal left and right, C3, C4 = Central left and right, O1, O2 = Occipital left and right, T7, T8 = Temporal left and right.

Journal Pre-proof